Master's Thesis

The novel effect of *Vernicia fordii* extract on insulin secretion in pancreatic β-cells and amelioration of insulin resistance in diabetic mice

Jimin Hyun

Department of Biological Sciences

Ulsan National Institute of Science and Technology

2021

The novel effect of *Vernicia fordii* extract on insulin secretion in pancreatic β-cells and amelioration of insulin resistance in diabetic mice

Jimin Hyun

Department of Biological Sciences

Ulsan National Institute of Science and Technology

The novel effect of *Vernicia fordii* extract on insulin secretion in pancreatic β-cells and amelioration of insulin resistance in diabetic mice

A thesis submitted to
Ulsan National Institute of Science and Technology
in partial fulfillment of the
requirements for the degree of
Master of Science

Jimin Hyun

12/18/2020
Approved by

_____

Advisor
Jang Hyun Choi

The novel effect of *Vernicia fordii* extract on insulin secretion in pancreatic β-cells and amelioration of insulin resistance in diabetic mice

Jimin Hyun

This certifies that the thesis of Jimin Hyun is approved.

12/18/2020

Signature

_____

Advisor: Jang Hyun Choi

Signature

_____

Jiyoung Park

Signature

_____

Young Chan Chae

Abstract

Vernicia fordii Hemsl. (*V. fordii*), also known as *Aleurites fordii*, is widely used in oriental medicine to treat wounds and infections. Diabetes is primarily caused by reduced secretion of insulin from pancreatic β-cells. Hence, the restoration of glucose-stimulated insulin secretion (GSIS) in the pancreas is effective therapy for type 2 diabetes. This study aimed to estimate the activity and mechanisms of *V. fordii* extract (VFE) as an insulin secretagogue and assess its potential as an antidiabetic agent. In pancreatic β-cells, VFE dramatically potentiated insulin release in a dose- & time-response manner and under hyperglycemia compared to euglycemia condition. Interestingly, the insulinotropic role of VFE was blunted by diazoxide and nifedipine. VFE significantly increased glucose uptake and ATP production, and stimulated PKCα/MARCKS activation by intracellular Ca^{2+} influx. Orally administered VFE ameliorated hyperglycemia and improved insulin sensitivity in HFD-fed mice, and reduced pancreatic islet size compared to that observed in HFD-fed mice. This study establishes that VFE has a strong insulinotropic effect and improves insulin sensitivity by increasing glucose uptake and PKCα activation *via* intracellular Ca^{2+} influx. Our study suggests that VFE could be potentially used for improving β-cell function and treating diabetes and metabolic diseases.

Keywords - *Vernicia fordii*, Glucose stimulated insulin secretion (GSIS), Intracellular calcium, Insulin sensitivity, Anti-diabetic action.

Contents

List of figures

List of tables

Abbreviations

2-NBDG : (2-deoxy-2-[(7-nitro-2,1,3-benzoxadiazol-4-yl) amino]-Dglucose)

ATP : Adenosine tri-phosphate

CREB : cAMP response element-binding protein

DAG : Diacylglycerol

Fura-2 AM : fura-2-acetoxymethyl ester

GSIS : Glucose stimulated insulin secretion

Glb : Glibenclamide

Glut2 : Glucose transporter 2

H&E : hematoxylin and eosin

HFD : High fat diet

HOMA-IR : Homeostatic Model Assessment for Insulin Resistance

IDF : International Diabetes Federation

IPITT : Intraperitoneal insulin tolerance test

Ins1 : Proinsulin gene 1

K_{ATP} : ATP sensitive K^+ channel

KRB : Krebs' ringer buffer

L-VDCC : L-type voltage-dependent calcium channel

MARCKS : Myristoylated alanine-rich C-kinase substrate

MIN6 : Mouse insulinoma 6

NCD : Normal chow diet

OCR : Oxygen consumption rate

OGTT : Oral glucose tolerance test

PC : Pyruvate carboxylase

PKCα : Protein kinase C α isoform

PLC : Phospholipase C

QUICKI: Quantitative insulin sensitivity check index

RLU : Relative luciferase units

RRP : Readily releasable pool

T1DM : Type 1 diabetes mellitus

T2DM : Type 2 diabetes mellitus

TG : Triglyceride

***V. fordii* :** *Vernicia fordii*

VFE : The 5^{TH} fraction divided by MPLC from *V.fordii* leaf methanol extract

I. Background

1-1. Type 2 diabetes mellitus

Type 2 diabetes mellitus (T2DM) is the ubiquitous people suffering metabolic disease which has been denoted in considerable areas of the world including western countries, Asia, and Africa (Fig. 1-1). T2DM accompanies lots of chronic and severe complications disturbing quality of life, such as cardiovascular disease (CVD), stroke, peripheral vascular disease like neuro- and retinopathy or End-stage renal disease. The healthcare costs for T2DM patients have been continuously increased and became a big burden on individuals and society [1].

T2DM, unlike type 1, is an acquired disease due to the lack of insulin action (Insulin resistance) with lower released insulin level (β-cell dysfunction) (Fig. 1-2), and is a progressive metabolic disease in which blood glucose continues to deteriorate even after the disease outbreak. T2DM is known to be caused by genetic factors or environmental such as a Westernization diet, sedentary lifestyle, and obesity [2].

1-2. Glucose-stimulated insulin secretion

In pancreatic β-cells, Glucose-stimulate insulin secretion (GSIS) is a chief insulin secretion system regulating the metabolic homeostasis of life. GSIS is led to the extracellular glucose elevation mediated glucose internalization *via* a glucose transporter. Internalized glucose participates in the oxidation system and intracellular ATP synthesis. Afterward, these changes induce blockage of the ATP sensitive K^+ channel occurs to the membrane depolarization resulting in intracellular Ca^{2+} influx, and consequently, insulin secretion by exocytosis aroused (Fig. 1-3) [3].

1-3. Natural products derived bioactive compounds treating diabetes

Due to its' diversity, the plant is a promising source of natural compounds that play a therapeutic role with lower risk in various diseases, and readily available [4]. Approximately, half percent of the US FDA approved drugs were the phytomedicinal derivatives such as metformin, aspirin, etoposide, teniposide, morphine, camptothecin, and quinine [5]. Furthermore, the tons of plants and derived bioactive-compounds have been detailed scientifically to be effective in treating T2DM, and studies have continued to search for highly active natural compounds for T2DM treatment (Fig. 1-4) [6]. However, these plants that are traditionally used as antidiabetic agents, their usage in diabetes treatment is limited due to a lack of research and proper tools for searching the mechanism of action. Burns *et al.*, have developed the easy and quick high-throughput screening tool using luciferase system for insulin secretagogues *in vitro* level [7]. Therefore, we used this analytical method for further study (Fig. 1-5).

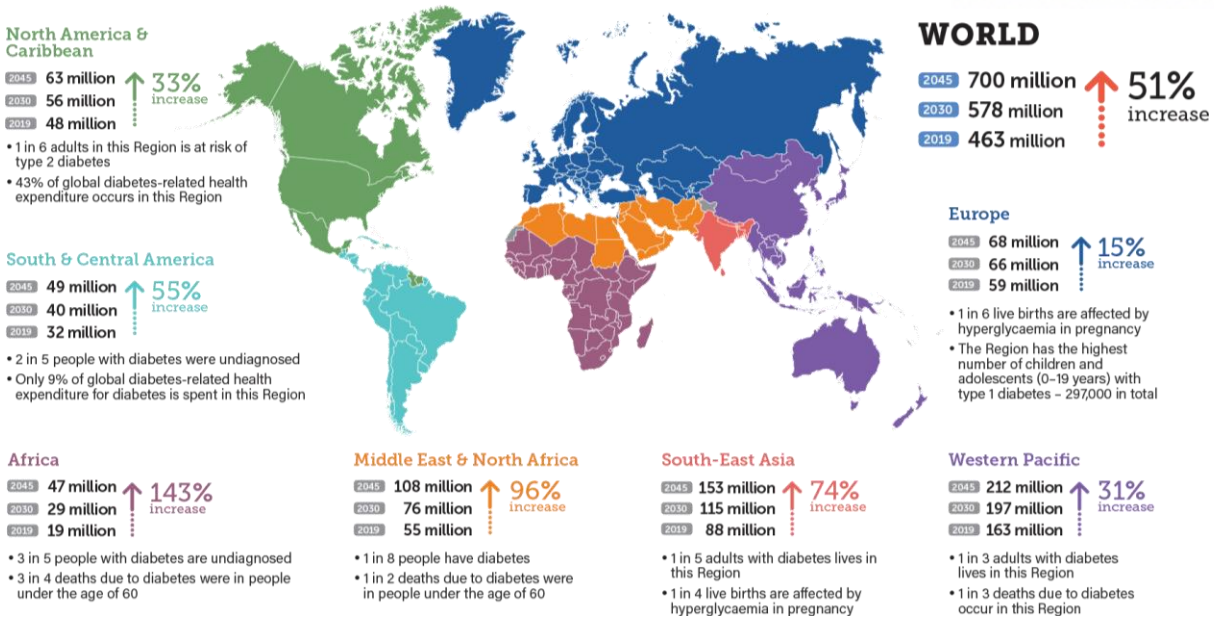

Figure 1-1. Number of adults suffering type 2 diabetes mellitus in the world (20-79 years)

IDF DIABETES ATLAS 9TH EDITION **(2019)**

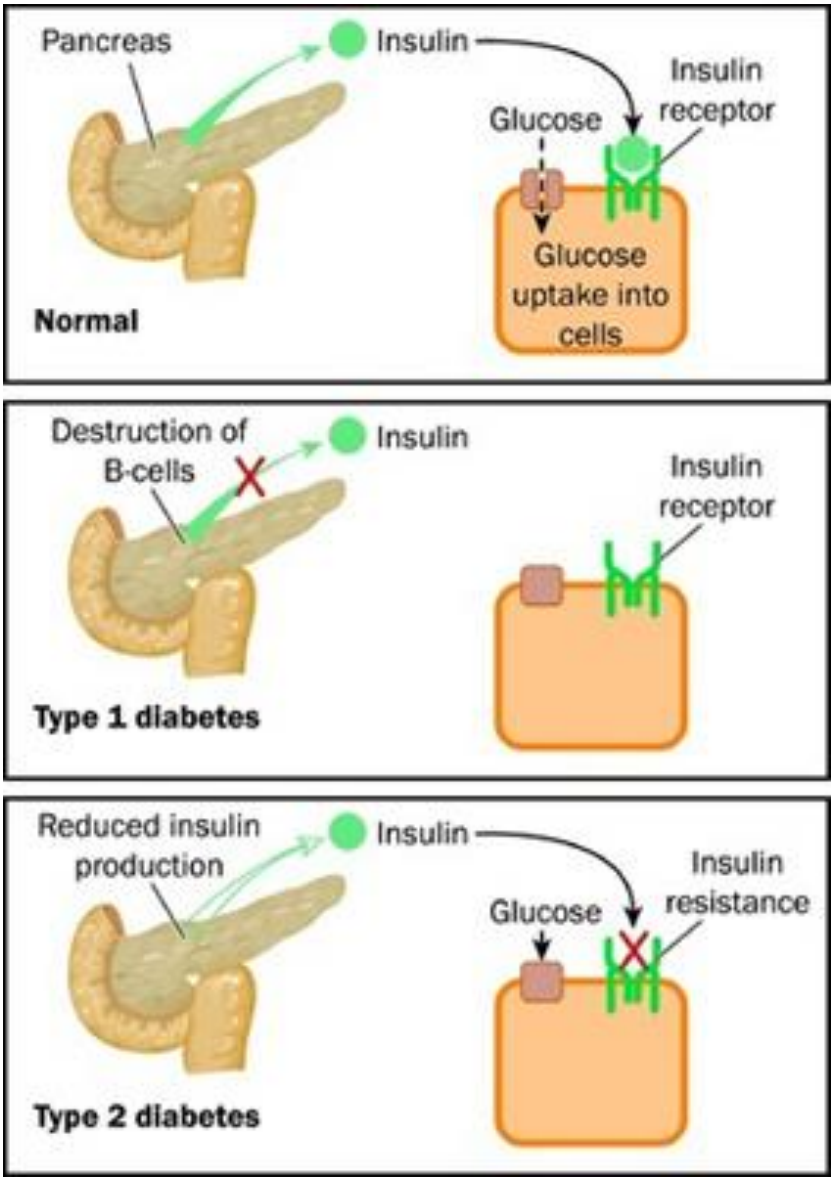

Figure 1-2. Major characteristics of pancreatic function in healthy *vs* diabetic individuals

Springer. Pancreatic Hormones and Control of Blood Glucose: A Glance. In: Diabetes Mellitus in 21st Century. **(2016)**

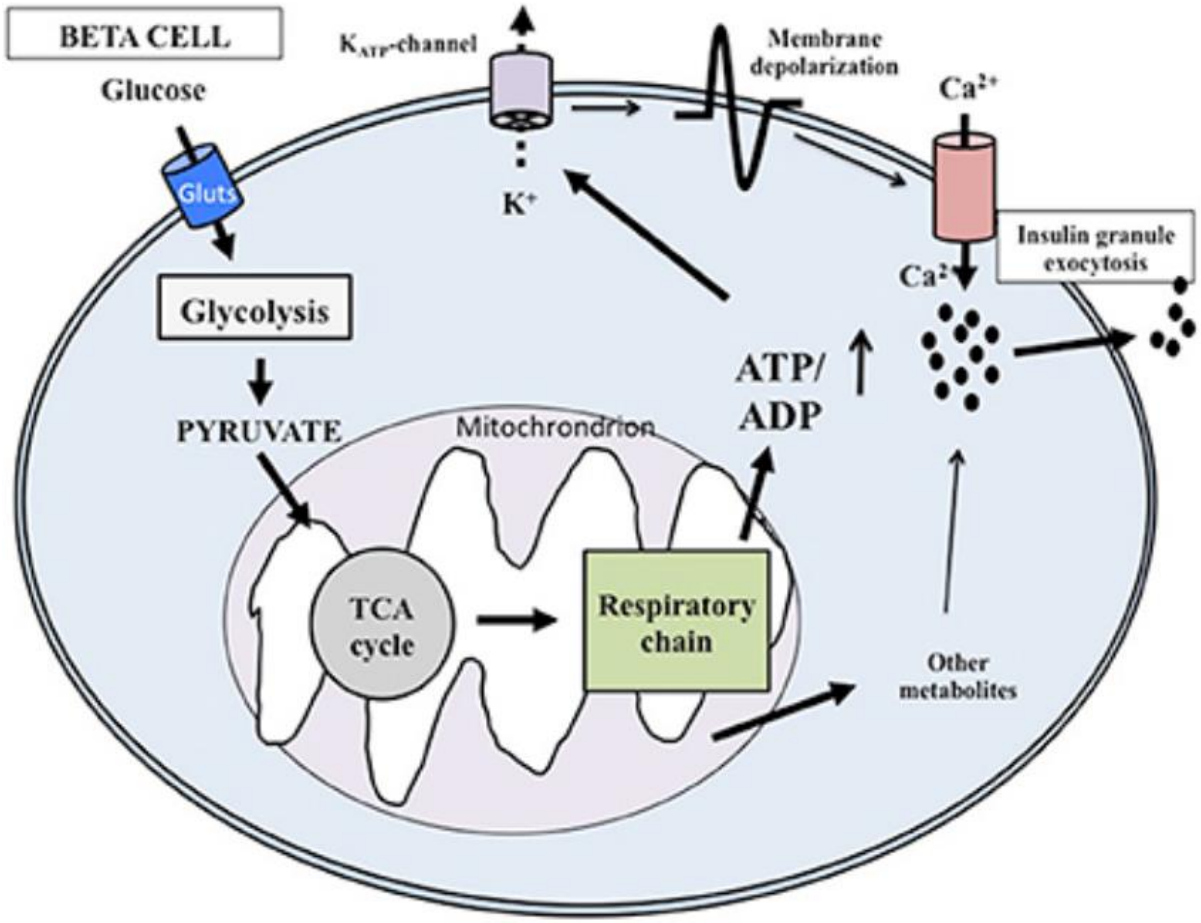

Figure 1-3. Glucose-stimulated insulin secretion mechanism

Front Cell Dev Biol. May 23;5:55 **(2017).**

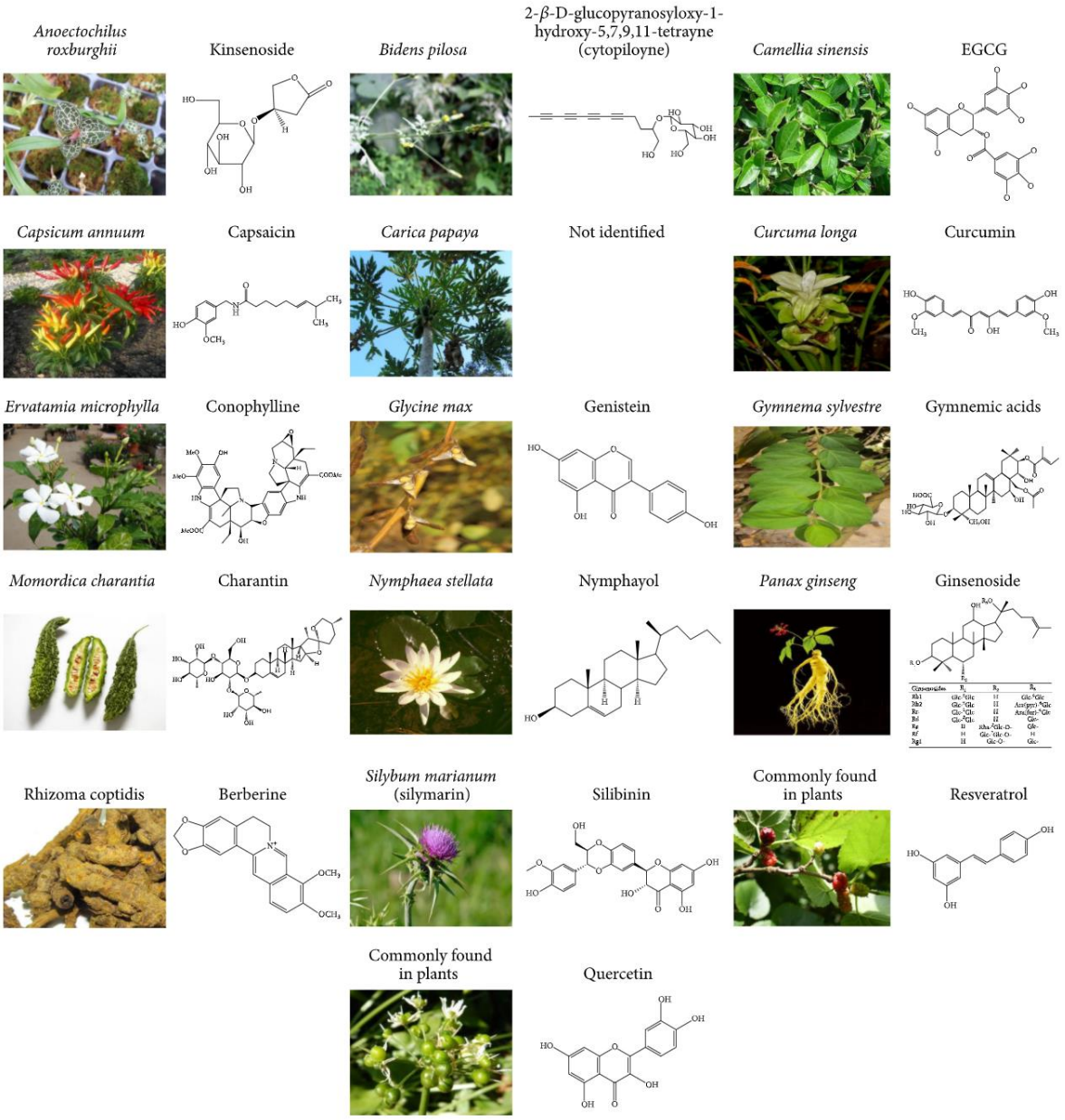

Figure 1-4. The characteristics of natural product improving pancreatic β-cell function and diabetes.

Hindawi Evid Based Complement Alternat Med 2015:629863; **(2015)**

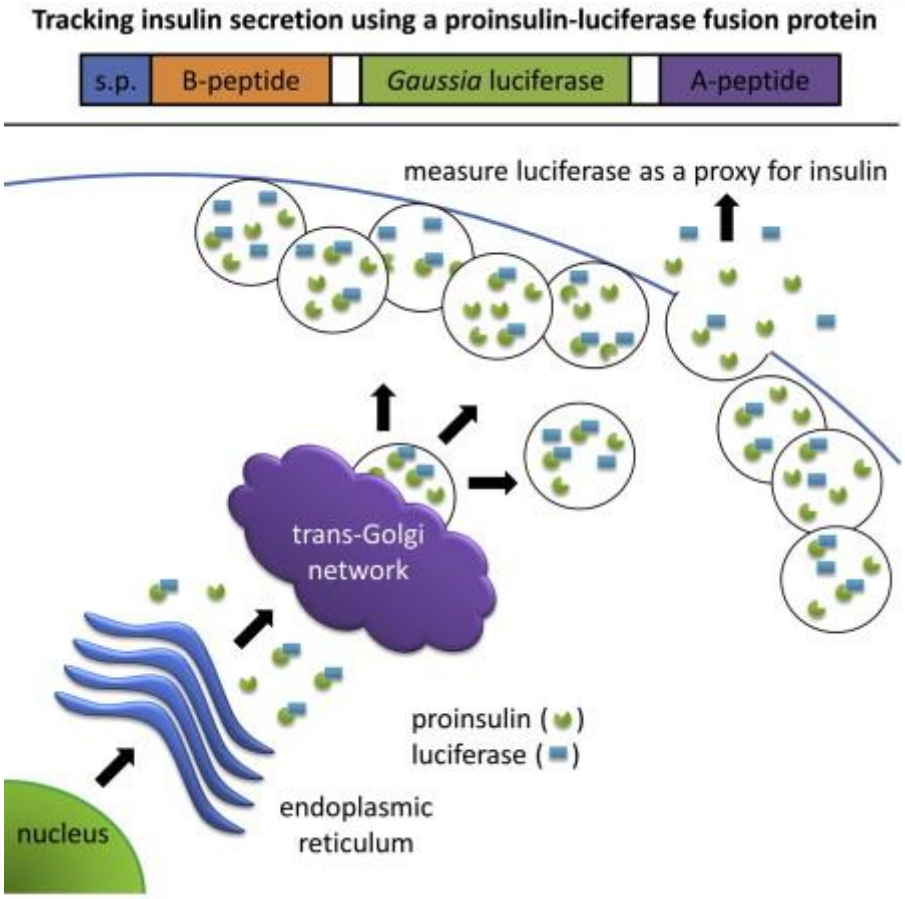

Figure 1-5. Luminescent insulin reporter assay by inserting *Gaussia* luciferase to pancreatic β-cells

Cell Met. Vol.21, *Issue 1*, 6 Jan, Pages 126-137 **(2015)**

1-4. Reference

1. DeFronzo, R. A.; Ferrannini, E.; Groop, L.; Henry, R. R.; Herman, W. H.; Holst, J. J.; Hu, F. B.; Kahn, C. R.; Raz, I.; Shulman, G. I.; Simonson, D. C.; Testa, M. A.; Weiss, R., Type 2 diabetes mellitus. *Nat Rev Dis Primers* **2015,** *1*, 15019.

2. LeRoith, D., Beta-cell dysfunction and insulin resistance in type 2 diabetes: role of metabolic and genetic abnormalities. *Am J Med* **2002,** *113 Suppl 6A*, 3s-11s.

3. Stumvoll, M.; Goldstein, B. J.; van Haeften, T. W., Type 2 diabetes: principles of pathogenesis and therapy. *Lancet* **2005,** *365* (9467), 1333-46.

4. Dias, D. A.; Urban, S.; Roessner, U., A historical overview of natural products in drug discovery. *Metabolites* **2012,** *2* (2), 303-336.

5. Kingston, D. G., Modern natural products drug discovery and its relevance to biodiversity conservation. *Journal of natural products* **2011,** *74* (3), 496-511.

6. Singh, J.; Cumming, E.; Manoharan, G.; Kalasz, H.; Adeghate, E., Suppl 2: Medicinal chemistry of the anti-diabetic effects of Momordica charantia: active constituents and modes of actions. *The open medicinal chemistry journal* **2011,** *5*, 70.

7. Burns, Sean M.; Vetere, A.; Walpita, D.; Dančík, V.; Khodier, C.; Perez, J.; Clemons, Paul A.; Wagner, Bridget K.; Altshuler, D., High-Throughput Luminescent Reporter of Insulin Secretion for Discovering Regulators of Pancreatic Beta-Cell Function. *Cell Metabolism* **2015,** *21* (1), 126-137.

II. *Vernicia fordii* extract stimulates insulin secretion in pancreatic β-cells

2-1. Introduction

Diabetes mellitus (DM), defined to prolonged hyperglycemia, is the most prevalent metabolic disease. DM, classified as type 1 or 2 (T1DM and T2DM), are innate and acquired disorders associated with pancreatic insulin secretion [8]. A major complication of diabetes is chronic hyperglycemia as a result of reduced insulin secretion from pancreatic β-cells [9]. In addition to reduced insulin secretion, peripheral tissues, such as liver, muscle, and fat tissues, fail to respond to insulin; this phenomenon is termed insulin resistance [8]. Impaired insulin secretion is a pathophysiological T2DM characteristic and causes diabetic vascular comorbidities (i.e.; neuropathy, retinopathy, and nephropathy) [10]. Therefore, restoring insulin secretion could be an effective strategy for treating hyperglycemia and diabetic complications.

Currently, various insulin-releasing drugs such as sulfonylureas, glucagon-like peptide (GLP-1) receptor agonists, and dipeptidyl peptidase-4 (DPP-4) inhibitors, were prescribed to T2DM patients have been prescribed limitedly owing to a series of severe side effects such as hypoglycemia, cardiovascular disease (CVD), and certain cancers [11]. Thus, antidiabetic drug development strategies should focus on controlling glucose homeostasis, thereby improving safety despite extended use.

In normal pancreatic β-cells, glucose metabolism is an essential process coupled to GSIS [12]. The transported glucose *via* glucose transporters is metabolically processed to generate the intracellular ATP. Increased level of ATP results in the closure of ATP-sensitive potassium ion channels (K_{ATP}). K_{ATP} channel blockade leads to membrane depolarization and subsequent opening of L-type voltage-dependent calcium channels (L-VDCCs), allowing Ca^{2+} influx, which stimulates insulin release. After the initial glucose-stimulated insulin secretion (first-phase), the altered intracellular Ca^{2+} level ($[Ca^{2+}]_i$) becomes a source for the lasting, intense insulin release (second-phase) from β-cells [12]. Among the second-phase insulin secretion associated signals, protein kinase C (PKC) roles critically in GSIS. Previous study identified that the activation of multiple PKC isoforms is closely associated with GSIS in β-cells. Particularly, glucose-induced $[Ca^{2+}]_i$ activates PKC, which phosphorylates various substrates involved in the second-phase release of insulin in β-cells [13]. In addition, this process potentiates susceptibility to Ca^{2+} response in exocytosis machinery, promoting the net released insulin in response to a given Ca^{2+} level [14].

Natural products are invaluable for the treatment of diseases [15]. Drugs sourced from natural products are considered safer, cheaper, easier to obtain and sometimes more effective for specific diseases than purely synthetic drugs. Particularly, active molecules from plants have been investigated as insulin secretagogues, and their role in the glycemic control of GSIS is being studied [16].

Vernicia fordii Hemsl. (*V. fordii*), also known as *Aleurites fordii*, is ubiquitously found in Korea and China. The leaves and fruit are used as an oriental treatment [17]. Recent studies identified the antiviral and anti-cancer effects of the active compounds derived from *V. fordii* leaf extracts [18, 19]. In particular, among the antiviral effects of *V. fordii*, the leaf extract and its refined derivatives act as an effective Epstein-Barr virus (EBV) lytic inducers in the gastric carcinoma cells (EBV-positive) *via* the PKC/MEK pathways [20]. However, the biological effects of *V. fordii* on glycemic control and insulin release have not been examined. Here, we demonstrated that the *V. fordii* leaf extract (VFE) had a strong insulinotropic effect in pancreatic β-cells and ameliorated insulin resistance. These findings reveal that VFE improves systemic insulin sensitivity and is a potential therapeutic candidate for T2DM.

2-2. Materials and Methods

Plant materials

Mass cultivated leaves parts of *Vernicia fordii* (*V. fordii*) were collected at Jeju-do, Republic of Korea, in June 2011 and identified by Dr. Chan-Soo Kim (Warm Temperature Forest Research Center, Korea Forest Research Institute), and a voucher specimen (KRIB 0000463) was deposited at the Plant Extract Bank (https://portal.kribb.re.kr/kpeb/) of KRIBB in Daejeon, Korea. After harvesting, the leaves were immediately freeze-dried (CleanVac 8 Hanil Science Medical, Korea), pulverized (tube mill, IKA, Germany) and stored at -40 ℃ until analysis.

Sample extraction and isolation

The leaves of *V. fordii* (343.6 g) were extracted in 100% methanol at room temperature for 24 h. The methanol extract of leaves of *V. fordii* (53.18 g, yield: 15.5 %, TVFE) was fractionated into five fractions using MPLC (Spot Prep II 250 instrument, Armen, France), which has assembled a reverse-phase silica gel column (YMC-Pack ODS-AQ-HG, 10 μm, 250×20 mm) under the conditions of a mobile phase in which water (A) and methanol (B) were mixed (0-10 min 10% B, 10-60 min 10-100% B, 60-90 min 100% B) and flow rate of 20 ml/min (Fig. 8. and 9.). For further bioactivity-guided fractionation, as a result of looking at increased insulin release in MIN6 cell for the separated five fractions, the highest insulin release was found in fraction 5 (VF Fr.5; VFE) (Fig. 2.B.). Based on this result, fractionation was continued for VFE, which was fractionated into seven fractions using the same equipment and columns from VFE, but different mobile phase conditions (A: water, B: MeOH, 0-5 min 60% B, 5-60 min 60-100% B, 60-100 min 100% B) (Fig. 8.-10.). The VF Fr. 5-3 (608 mg) was fractionated into 14 fractions using Gilson PLC 2250 Purification System (WI, USA) assembled a reversed-phase silica gel column (INNO C18, 5 μm, 250×20 mm) under the conditions of a mobile phase in which water with 0.1% trifluoroacetic acid (A) and acetonitrile (B) were mixed (0-5 min 75% B, 5-60 min 75-85% B, 61-70 min 100% B) and flow rate of 17 ml/min (Fig. 8.-13.). The VFL Fr. 5-3-9 (94.9 mg) was isolated for 12-O-hexadecanoyl-16-hydroxyphorbol-13-acetate (HHPA, 9.7 mg) using Gilson PLC 2250 Purification System assembled a reversed-phase silica gel column (synergy polar, 4 μm, 250×20 mm) under the conditions of a mobile phase in which water with 0.1% trifluoroacetic acid (A) and acetonitrile (B) were mixed (0-5 min 60% B, 5-60 min 60-70% B, 61-70 min 100% B) and flow rate of 15 ml/min (Fig. 8.-16.). The yield of the HHPA obtained was 0.21% from MeOH extract determined by using ultra-performance liquid chromatography (UPLC) charged with photodiode array (PDA) and charged aerosol detector (CAD) (Fig. 8.-17.). Based on UPLC-CAD analysis, the purity of HHPA was more than 97.0% (Fig. 8.-18.). HHPA was tentatively identified by UV, MS and MS/MS spectra, and HRMS of HHPA compared of the previous literature data, including the UV, *m/z* values, MS fragments, and molecular formulae data [21] (Fig. 7. and Table 1.). The main compound (9.7 mg)

were dissolved in 600 µl chloroform-*d* (Cambridge Isotope Laboratories, MA, USA) as a solvent, with tetramethylsilane (TMS) as an internal standard, and then measured to NMR (Bruker AVANCE III HD 700 MHz, MA, USA). Chemical shifts were reported in ppm (δ) and J in Hz values. HHPA were identified by comparisons of chemical shifts previously reported (Fig. 19.-20., and Table 2-3) [20-22].

Cell Culture

The mouse pancreatic β-cell line MIN6 was gifted from Prof. Jun-Ichi Miyazaki (Osaka University, Japan). Unless otherwise indicated, entire chemical materials were supplied from Sigma-Aldrich (MO, USA) for cell culture. Primary islet was isolated using the methods which was published in previous report (Hwang et al., 2018). MIN6 cells were cultured in Dulbecco's Modified Eagle Medium (DMEM) and the isolated islets were cultured in RPMI-1640 medium. Both medium was containing with 10% fetal bovine serum (Gemini Bio-products, CA, USA), 55 µM β-mercaptoethanol, 2 mM L-glutamine, 1% penicillin/streptomycin (Thermo Fisher Scientific, MA, USA). Cells were cultured at 37 ℃ in a humidified air containing 95% air and 5% CO_2.

Insulin secretion assay

Proinsulin-NanoLuc in pLX304 plasmid for Luminescent reporter of insulin secretion assay was purchased from Addgene (MA, USA). Proinsulin-*Gaussia* luciferase analysis was performed using the methods which were previously reported (Burns et al., 2015). Briefly, proinsulin-*Gaussia* luciferase plasmid-introduced MIN6 cells and incubation in 96-well scale for 72 h. Prior to luciferase analysis experiments, MIN6 cells were rinsed with PBS and supplemented 2.8 mM glucose containing Krebs Ringer bicarbonate buffer (KRB). After 1 h, MIN6 cells were applied with KRB containing different doses of chemicals with 2.8 or 16.7 mM glucose for another 1 h. Size-matched primary islets were applied to the indicated concentration of chemicals in KRB with 2.8 or 16.7 mM glucose for additional 1 h. As the vehicle, DMSO was treated. The amount of insulin in each supernatant from MIN6 and pancreatic islets were quantified to coelenterazine substrate addition (Nanolight Tech., AZ, USA) and ELISA (Alpco Diagnostics, NH, USA), respectively. All steps were performed in a 37 ℃, 5% CO_2 incubator.

***In vitro* cytotoxicity test**

For analyzing the cytotoxic effect of VFE on MIN6 cells, we carried out the MTT (3-(4,5-dimethylthiazol-2-yl)-2,5-diphenyl tetrazolium bromide) test former reported [23].

Glucose uptake measurement

Uptake glucose levels were measured in MIN6 cells with a 2-[N-(7-nitrobenz-2-oxa-1,3-diazol-4-yl)amino]-2-deoxy-D-glucose (2-NBDG, Cayman Chemical). MIN6 cells were rinsed and maintained for 1 h at 37 °C in glucose-free KRB. Subsequently, 600 µM 2-NBDG has applied to the

cells with VFE for 20 min at 37 °C. To eliminate the debris or background fluorescence, the cells were then rinsed two times with free glucose KRB and added Lysis buffer [(mM) 150 NaCl, 50 Tris-HCl (pH 8.0), 5 EDTA, 1% Triton X-100, 0.1% SDS, with 0.5% Na-deoxycholate] to detect the fluorescent intensity using a microplate reader (Tecan Trading) at 485/535 nm. Fluorescence intensity was normalized by the protein amounts per each well after background subtraction.

Mitochondrial oxygen consumption rate (OCR)

The effect of VFE on mitochondrial function was assessed from MIN6 cells in XFe24 microplates (Seahorse Bioscience, MA, USA). The cells were treated with VFE in 16.7 mM glucose KRB for 1 h following 2.8 mM glucose containing KRB incubation for 1 h. Then, cells were rinsed with extracellular flux modified medium (Seahorse Bioscience). Then the plate was performed to a Seahorse Bioscience XFe24 extracellular flux analyzer, and Oligomycin (2 μM), FCCP (3 μM), Rotenone (1 μM) were consequently applied to evaluate the OCR for 2 h in MIN6 cells. Entire chemicals were purchased from Sigma-Aldrich.

Intracellular Ca^{2+} measurement

PBS rinsed MIN6 cells were stained using 10 μM Fura-2AM (fura-2-acetoxymethyl ester; Invitrogen, CA, USA) in glucose-free KRB during 30 min. The cells were then rinsed again by glucose-free KRB and loaded onto a microscope holder. The chemicals were applied to the cells on image screened by the mixture. The excitation was detected by a fluorimeter to monitor Fura-2AM at difference fluorescence 340 / 380 nm simultaneously using Olympus IX81 microscope (Olympus Corp., Japan).

Western blot analysis

MIN6 cells stimulated by VFE or tissues from VFE-treated mice were treated with RIPA buffer (Thermo Fisher). Quantified protein was applied to SDS-PAGE and transferred to nitrocellulose membrane (GE healthcare, CA, USA). 5% (w/v) bovine serum albumin was used for the blocking the membrane and the membrane was incubated with primary antibodies overnight at 4 ℃. Anti-Phospho-PKC Substrate Motif [(R/K)XpSX(R/K)] MultiMab™ rabbit mAb mix, anti-phospho-MARCKS (S152/156), anti-phospho-Akt (S473), anti-Akt, anti-phospho-CREB (S133), anti-CREB, anti-β-Actin, and anti-HSP90 antibodies were purchased from Cell Signaling (MA, USA). Anti-phospho-PKCα (S657), anti-PKCα, anti-MARCKS antibodies were purchased from Santa Cruz Biotechnology (TX, USA). We assessed the intensity of band by ImageJ (NIH, MD, USA).

Gene expression analysis

Extraction of RNA as of cells and tissues was carried out using Trizol (Invitrogen, CA, USA). The complementary DNA which was synthesized by reverse-transcription kit (ABI; Invitrogen) was

used to quantitative PCR with SYBR dye (ABI9300; Thermofisher). Relative mRNA expressions estimated by the ΔΔ-Ct equation were divided to ribosomal Protein L32 (*Rpl32*) expressions. Primers for each gene were summarized in the Table 4.

Animal experiments

Entire *in vivo* experiments were followed the Ulsan National Institute of Science and Technology's Institutional Animal Care and Use Committee (UNISTIACUC-19-04). Wild C57BL/6J mice were cared in the pathogen-free facility under 12-h light/dark cycles. Standard diet with water was given to *ad* libitum. For 16 h, C57BL/6J male mice (8-week-old) were restricted to diets. Mice were orally injected 3 g/kg D-glucose after 30 min 10, 20, or 50 mg/kg doses of VFE, and 30 mg/kg dose of Glbenclamide, or vehicle oral administration. The monitoring of blood glucose was performed by tail blood using glucometer (All Medicus, Korea), and Mouse Ultrasensitive Insulin ELISA (ALPCO) kit was used for serum insulin detection.

For analyzing metabolic effects of VFE, the male C57BL/6J mice (8-week-old) were received high-fat diets (HFD) (60% kcal fat, D12492, Research Diets Inc., NJ, USA) during 4-weeks and orally supplied 20 or 50 mg/kg VFE, and 30 mg/kg Glb, or vehicle for additional 6-weeks with HFD. Body and intake food weights were checked in every week. For oral glucose tolerance test (OGTT), mice were restricted food for 16 h before 3 g/kg d-glucose injection. The mice restricted food for 6 h were received 0.75 U/kg insulin intraperitoneal injection for intraperitoneal insulin tolerance test (IPGTT). The blood glucose were monitored by glucometer (All Medicus). HOMA-IR was acquired following the previous report [24]. QUICKI was acquired using the equation (QUICKI = 1 / [log(FI[μU/ml]) + log(FG[mg/dl])]). Serum insulin (ALPCO) and TG (Cayman chemical) were determined by ELISA.

Histological analysis

Whole pancreas is collected and fixed using 4 % paraformaldehyde overnight at RT. The fixed pancreas was subsequently dehydrated and embedded in paraffin. The paraffin blocks were sectioned with a DM6000B microtome (Leica, Germany). To dewax the sections, each tissue section was exposed to the sequential steps of xylene and ethanol washes. Tissues were counterstained with H&E to represent pancreatic islet structures.

Statistical analysis

Data are shown as means + S.E.M. The estimated statistical significance using unpaired t-test was compared within paired condition. The comparison between more than two conditions was used a one-way ANOVA. Dunnett's post hoc test was tried multiple comparisons. GraphPad Prism 8.0 software was used for entire statistics (GraphPad, CA, USA).

2-3. Results

***V. fordii* extract (VFE) increases insulin secretion in hyperglycemic conditions**

To search the effect of *V. fordii* on the function in pancreatic β-cells, we performed a luminescent reporter assay using Proinsulin-*Gaussia* luciferase construct inserted MIN6 cells. In the low glucose condition (2.8 mM glucose; LG), TVFE, the *V. fordii* leaf methanol extract, did not increase insulin secretion (0.3 μg/ml; 1.11 ± 0.36, 1.25 μg/ml; 1.15 ± 0.11, and 5 μg/ml; 1.20 ± 0.19 fold increases) (Fig. 1.A.). In contrast, under high glucose condition (16.7 mM glucose; HG) TVFE resulted in significant increase in insulin secretion dose-dependently (0.3 μg/ml; 2.06 ± 0.03, 1.25 μg/ml; 3.44 ± 0.16, and 5 μg/ml; 6.05 ± 0.29 fold increases). In addition, insulin release stimulated by TVFE was similar to that of 12-*O*-Tetradecanoylphorbol-13-acetate (PMA) which reportedly increases insulin secretion in pancreatic β-cells [13]. Next, we fractionated TVFE, producing VFE as the most effective fraction in stimulating insulin secretion in MIN6 cells (Fig. 1.B.). MIN6 cells with VFE incubation potentiated insulin release in a dose-dependent manner in HG (0.1 μg/ml; 4.44 ± 0.23, 0.3 μg/ml; 6.29 ± 0.38, 1 μg/ml; 7.90 ± 0.55, and 500 nM PMA; 9.11 ± 0.10 fold increases) (Fig. 1.C.). Besides, VFE stimulated insulin release, which was significant starting from 15 min after treatment and reached a maximum 1 h after treatment in MIN6 cells (Fig. 1.D.). Consistent with the results in MIN6 cells, VFE significantly increased insulin release in a dose-responsibly in murine primary islets; this effect on insulin release was more dramatic under HG conditions (0.1 μg/ml; 3.41 ± 0.42, 0.3 μg/ml; 5.25 ± 0.31, 1.0 μg/ml; 10.18 ± 0.24 %, 500 nM PMA; 16.61 ± 0.56 fold increases) (Fig. 1.E.). To validate the cytotoxic effect of TVFE or VFE in the MIN6 cells, we performed an MTT assay. Cell viability was not altered at concentrations <20 μg/ml of each chemical, indicating that TVFE and VFE potentiate insulin release without inducing cytotoxicity (Fig. 1.F.), Thus, these data suggest that VFE potentiates GSIS in pancreatic β-cells.

VFE increases intracellular Ca^{2+} influx in MIN6 cells

The rise of intracellular Ca^{2+} level ($[Ca^{2+}]_i$) is essential for GSIS *via* activation of exocytosis [12]. As VFE stimulated insulin secretion in HG compared to LG, we hypothesized that VFE-induced insulin secretion is mediated by increased $[Ca^{2+}]_i$. We measured the acute Ca^{2+} transition after VFE treatment during Fura-2AM loading in MIN6 cells. As shown in Fig. 2.A. and 2.B., a substantial elevation in the $[Ca^{2+}]_i$ was monitored following VFE treatment in a dose-dependent manner. Glibenclamide (Glb), a specific inhibitor of K_{ATP} sulfonylurea receptor 1 channels (Sur1-Kir6.2) that is used either as monotherapy or in combination with biguanides in the management of T2DM was used as a positive control to increase $[Ca^{2+}]_i$ [25].

Next, we determined whether the sources of Ca^{2+} was extra- or intracellular. In the absence of extracellular Ca^{2+} ($[Ca^{2+}]_e$), the use of calcium-free KRB buffer resulted in a dramatic reduction in VFE-

induced GSIS compared with that observed on using Ca^{2+} containing KRB (Fig. 2.C.). These results propose that VFE on insulin release is largely on account of the $[Ca^{2+}]_e$ influx in pancreatic β-cells.

VFE activates PKCα-MARCKS for insulin secretion.

It is established that increased $[Ca^{2+}]_i$ triggers PKCα activation, which is a key mechanism for inducing GSIS in pancreatic β-cells [13, 26]. Thus, we tested whether VFE activates PKC in pancreatic β-cells. As shown in Fig. 3.A. and 3.B., VFE dramatically increased PKC activation in dose- and time-response manner, as confirmed by western blotting with PKC substrate antibody or phospho-specific PKCα antibody. In addition, we confirmed that VFE activated myristoylated alanine-rich C-kinase substrate (MARCKS), the major PKC substrate that is involved in insulin secretion by actin rearrangement in pancreatic β-cells (Fig. 3.A. and 3.B.) [27]. The specific inhibitor of PKC, Gö6983 significantly inhibited the activation of both PKCα and MARCKS (Fig. 3.C.), and insulin secretion (Fig. 3.D.). Beside increased $[Ca^{2+}]_i$, it is reported that PKCα can be activated by phospholipase C (PLC) stimulation [26]. Thus, we checked whether VFE alternatively activates PKCα *via* PLC activation. As shown in Fig. 3.E., the insulinotropic effect of VFE did not be changed by a specific inhibitor of PLC, U73122 in MIN6 cells, indicating that VFE stimulates insulin secretion mainly through Ca^{2+}-induced PKCα activation.

Thereafter, we investigated whether the disruption of $[Ca^{2+}]_e$ influx or K_{ATP} activation regulates PKCα activation and insulin release in pancreatic β-cells. It has been well studied that $[Ca^{2+}]_e$ inflow through either L-VDCCs or K_{ATP} is crucial to insulin secretion [12]. The inhibition of L-VDCCs by nifedipine, a specific L-VDCC blocker, suppressed VFE-induced PKCα activation and insulin secretion, indicating that the $[Ca^{2+}]_e$ inflow *via* L-VDCCs by VFE increases insulin exocytosis (Fig. 3.F. and 3.G.). Furthermore, the selective K_{ATP} activator diazoxide reduced PKCα activation and insulinotropic effect of VFE (Fig. 3.H. and 3.I.). Thus, these data strongly suggest that $[Ca^{2+}]_e$ influx *via* L-VDCCs and K_{ATP} channels by VFE treatment is critical for insulin exocytosis *via* Ca^{2+}-dependent PKCα activation in the pancreatic β-cells.

VFE promotes glucose uptake and mitochondrial ATP production

Glucose transport and metabolism in pancreatic β-cells are essential process coupled to GSIS by the regulation of K_{ATP} activity [12]. Thus, we investigated the effect of VFE on GSIS by measuring intracellular glucose abundance and mitochondrial ATP production. First, glucose uptake estimated by 2-NBDG revealed that VFE dramatically enhanced glucose transport into MIN6 cells in a dose-dependent manner (Fig. 4.A.). In murine pancreatic β-cells, the major glucose transporter is *slc2a2* (also known as glucose transporter-2; Glut2) [28], therefore, we analyzed the expression of Glut2 in the presence with VFE. As shown in Fig. 4.B., VFE rose notably the Glut2 expresion. In addition to Glut2, the expression of *Pcx* (Pyruvate carboxylase; PC) and *Ins1* (proinsulin gene 1; Ins1) which have prominent

roles in GSIS also increased after treatment with VFE (Fig. 4.B.). Reportedly, the expression of Glut2, PC, and Ins1 are tightly regulated by the cAMP response element-binding protein (CREB) activity [29]. As shown in Fig. 4.C., the activation of CREB by VFE was dose-dependent, indicating that VFE enhances CREB activity and CREB-mediated gene expression to promote glucose uptake in pancreatic β-cells.

Next, we estimated the effect of VFE on mitochondrial respiration using a seahorse cellular bioenergetic analyzer. Oligomycin A (a complex V inhibitor), carbonyl cyanide-4-trifluoromethoxyphenylhydrazone (FCCP) (an oxidative phosphorylation uncoupler), and rotenone (a complex I inhibitor) were sequentially added to evaluate the effect of VFE on the electron transport chain function. Pre-treatment with VFE dramatically increased the oxygen consumption rate (OCR) in a dose-response manner (Fig. 4.D.). The basal respiratory rate and the FCCP-treated maximal capacity of mitochondrial respiration were both increased by VFE (Fig. 4.E.). Finally, the increased OCR by VFE resulted in increased ATP generation in MIN6 cells dose-dependently (Fig. 4.F.). These data support the notion that the boosted mitochondrial function including enlarged glucose uptake and ATP generation, is a vital mechanism for VFE-stimulated insulin secretion in MIN6 cells.

VFE reduces blood glucose level through insulin release promotion *in vivo*

To explore the insulinotropic effect of VFE *in vivo*, we performed the VFE pre-treatment to male C57BL/6J mice (8-week-old) in various doses *via* oral injection followed by glucose administration and monitoring of blood glucose levels. The dose-dependent glucose-lowering effect of VFE was observed at 30 min after glucose administration during an oral glucose tolerance test (OGTT) (Fig. 5.A.). VFE-injected mice showed a remarkable glucose decrease in blood in comparison to vehicle-treated mice (VFE 10 mg/kg, 19.9 ± 4.1 %; 20 mg/kg, 31.3 ± 1.7 %; 50 mg/kg, 38.6 ± 1.1 % reduction). Glb significantly reduced blood glucose levels (49.8 ± 2.2 % reduction), as reported [25]. Despite neither VFE nor Glb altering the body weight (Fig. 5.B.), the VFE induced blood glucose reduction was attended with an increased level of plasma insulin after glucose administration (Fig. 5.C.). These results show that the VFE glucose-lowering effect is the result of promoted insulin secretion in pancreatic β-cells.

VFE improves insulin sensitivity in HFD-induced diabetic mice

Impaired insulin secretion is a critical pathophysiologic character of T2DM and the restoration of insulin secretion is an effective therapeutic options for diabetic complications [30]. Since observing the promising insulinotropic effect of VFE with lowering blood glucose levels, we investigated whether VFE exerts antidiabetic properties *in vivo*. We orally injected VFE at indicated doses for additional 6-weeks in the same diet after feeding a high fat diet (HFD) to wild-type C57BL/6J mice for 4-weeks. As shown in Fig. 6.A., compared with normal chow diet (NCD)-fed mice, HFD-fed mice exhibited substantial bodyweight gain. However, either VFE or Glb did not change the bodyweight or food intake

compared with vehicle treatment in HFD-fed mice (Fig 6.A. and 6.B.). Surprisingly, VFE administration for 5-weeks dramatically reduced fasting blood glucose levels, as did Glb, indicating that VFE has a potent hypoglycemic effect (Fig. 6.C.).

After 6-weeks' oral administration of VFE in HFD-fed mice, we performed an OGTT and IPITT. VFE dramatically alleviated the glucose intolerance and insulin resistance of HFD-fed mice and improved the fasting glucose levels in a dose-dependent manner (Fig. 6.D. and 6.E.). Control mice that supplied vehicle only had hyperinsulinemia, but VFE substantially lowered the fasting insulin levels in these mice (Fig. 6.F.). Decreased levels of HOMA-IR and increased levels of QUICKI clearly showed an improvement of insulin sensitivity following treatment with VFE (Fig. 6.G. and 6.H.). In addition, serum triglyceride (TG) levels remarkably decreased in VFE-treated mice, suggesting that VFE ameliorates insulin sensitivity in the fat tissue of VFE-treated mice (Fig. 6.I.).

In addition, the major glucose-consuming peripheral tissues, such as liver and muscle exhibited activation of AKT which may indicate the glucose clearance effect on VFE fed mice compared with the diabetic control (Fig. 6.J.). Pancreatic islet expansion, especially β-cell mass, is well established in long-term HFD feeding studies [31, 32]. As shown in Fig. 6.K., H&E staining of the pancreas revealed that HFD dramatically increased β-cell mass compared to NCD, and VFE significantly reduced the size of pancreatic islets compared to HFD-fed group (Fig. 6.K.). These data suggest that VFE improves insulin sensitivity and prevents diabetic progression.

Analysis of the major constituents of *V. fordii* leaves

To isolate and identify the compounds of the *V. fordii* for increase in insulin release, a preliminary literature review and bioassay-guided fractionation were performed. A methanol extract was prepared from the leaves of *V. fordii* (TVFE) and was divided into 5 fractions (VF1–5) using MPLC. VF fraction 5 (VFE) showed significantly higher activity than the other fractions (Fig. 1.B.). Bioassay-guided fractionation of the extract afforded a more active TVFE and VFE containing a variety of tigliane diterpene esters, as revealed by ultraperformance liquid chromatography quadrupole time-of-flight mass spectrometry (UPLC-QToF-MS) analysis (Fig. 7.A.). Searching the mass to charge ratios (*m/z*) of precursor ion using a published MS results-based approach and LCMS-guided isolation, led to the separation of four structurally unique tigliane diterpene esters. The exact molecular ions of the four peaks were 689 $[M–H]^-$, 705 $[M–H]^-$, 673 $[M–H]^-$, and 643 $[M–H]^-$ (Table. 1). The most active fractions 5-3 and 5-3-9 which were divided from VFE using the prep-HPLC, were screened insulin secretion effect in MIN6 cells for searching the effective compounds (Fig. 11. and 14.). The compounds were discovered by comparing the spectroscopic data, including 1D-NMR, HRMS, calculated mass, error ppm, and chemical formula, with those previous reported [20, 22]. Finally, we identified four compounds in VFE: 12-*O*-hexadecanoyl-16-hydroxyphorbol-13-acetate (HHPA), 12-*O*-hexadecanoyl-7-oxo-5-ene-16-hydroxyphorbol-13-acetate, 12-*O*-hexadecanoyl-4-deoxy-4α-16-hydroxyphorbol-13-

acetate, and 12-*O*-hexadecanoyl-phorbol-13-acetate (Fig. 7.B.).

2-4. Discussion

Impaired insulin production is a typical feature of T2DM. Controlling postprandial blood glucose levels by either insulin analogs or endogenous insulin-releasing molecules is an effective treatment for T2DM. However, hypoglycemic control through insulin analogs may increase the risk of developing diseases, such as bacterial infection, insulin autoimmune syndrome (IAS), or Hirata's disease [33]. Therefore, regulation of blood glucose levels through enhanced endogenous insulin secretion is a more effective and safer therapy for the treatment of T2DM. Although insulin secretagogues such as sulfonylurea are broadly prescribed to promote insulin secretion in T2DM patients, continuous drug treatments are restricted due to side effects, for instance hypoglycemia, weight gain, and CVD [11]. Thus, the development of novel insulin secretagogues has been focused on characterizing natural compounds. It has been reported that *V. fordii* is widely used as a suppressing viral infection and cancer progression in China [19, 34]. Despite the identification of numerous phytochemicals of *V. fordii*, there is no evidence that they regulate insulin secretion and systemic insulin sensitivity. In this study, we illuminated that VFE has a potent role in pancreatic β-cells for insulin production *in vitro* and *in vivo*. These effects of VFE contribute to improvement in glucose tolerance and insulin action in a mouse model of diabetes.

Insulin is secreted from pancreatic β-cells to the biphasic process [12]. After elevation of glucose level, a transient increase in insulin occurs (first-phase secretion; within 15 min of glucose stimulation). Thereafter, the second-phase secretion follows, presumably due to a metabolic amplification pathway involving increased $[Ca^{2+}]_i$[35]. We showed that VFE regulates first- and second-phase secretion of insulin in MIN6 cells in this study. VFE dramatically increased $[Ca^{2+}]_i$ within 2 min and insulin secretion was significantly increased within 15 min after VFE application (Fig. 1.D.). In addition, VFE-induced insulin secretion was amplified by Ca^{2+}-dependent PKCα activation, which performs a staple part in second-phase insulin release in pancreatic β-cells (Fig. 3.A. and 3.B.). Reportedly, only fuel such as glucose can lead to second-phase insulin secretion through amplifying pathway, and it has been known that non-metabolized stimuli can cause to only first-phase insulin secretion [12]. We demonstrated that VFE potentiates glucose uptake in pancreatic β-cells, implying that VFE modulates second-phase insulin secretion which is a glucose-dependent process.

With extended purification analysis of VFE, we identified four compounds; 12-*O*-hexadecanoyl-16-hydroxyphorbol-13-acetate (HHPA), 12-*O*-hexadecanoyl-7-oxo-5-ene-16-hydroxyphorbol-13-acetate, 12-*O*-hexadecanoyl-4-deoxy-4α-16-hydroxyphorbol-13-acetate, and 12-*O*-hexadecanoyl-phorbol-13-acetate as the bioactive constituents to stimulate GSIS in MIN6 cells (Fig. 8.A. and 8.B.). Among them, HHPA exhibited the strongest effect on GSIS, which is structurally comparable to PMA, but is non-toxic (Fig. 21.-22.). Although HHPA is a PMA analog, it is possible that HHPA has different modes of action in GSIS than PMA. First, PMA is reported to activate PKCα to stimulate insulin secretion [36]. However, the enhanced secretion by PMA did not alter glucose

metabolism, K_{ATP} activity, or $[Ca^{2+}]_e$ influx [37]. Our results strongly suggest that VFE upregulates the mitochondrial function through increased glucose uptake and increases Ca^{2+} influx in MIN6 cells (Fig. 2.A. and 2.B.). In addition, we demonstrate that K_{ATP} inhibition due to ATP augmentation stimulated by VFE is an important mechanism for insulin secretion in MIN6 cells (Fig. 3.H. and 4.F.). Secondly, it is reported that staurosporine, a potent PKC inhibitor, completely suppressed PMA-induced insulin secretion [27]. However, it could partially block GSIS as well, suggesting that staurosporine directly inhibits PKC, and alternative pathways could be involved in GSIS [38]. Thirdly, besides $[Ca^{2+}]_i$, DAG which is produced by PLC, is involved in the activation of PKCα. As PMA can mimic DAG to induce insulin secretion in pancreatic β-cells, we tested the effect of PLC on VFE-mediated insulin secretion. However, the selective PLC inhibition did not alter VFE-induced insulin release. These results represent that the $[Ca^{2+}]_i$/PKCα axis not DAG, is the main target mechanism of VFE (Fig. 3.E.).

In pancreatic β-cells, GSIS is regulated by several key genes, such as *Glut2*, *Ins1*, and *PC*. A lack of glucose transporter has been reported in murine T2DM models and human T2DM patients, and its deficiency in the pancreas resulted in a loss of GSIS, leading to severe hyperglycemia [39]. Insulin hormone encoding *Ins1* gene plays essentially in insulin biosynthesis and insulin production [40]. Previous results have shown that chronical high glucose exposure to β-cells is related to blunted precursor insulin biosynthesis and lower *Ins1* gene expression level [41]. Pyruvate carboxylase (PC), a key enzyme of tricarboxylic acid (TCA) cycle in mitochondria, is abundantly expressed in β-cells. It is suggested that in pancreatic β-cells, the PC pathway plays an important role in pyruvate metabolism, insulin release and cell proliferation [42]. Thus, the alteration of these gene expressions in pancreatic β-cells is a hallmark of T2DM. Similar to these results, we checked that VFE rose the Glut2, Ins1, and PC expressions coupled with glucose-dependent CREB activation (Fig. 4C). and mitochondrial function (Fig. 4.D.-4.F.). The elevation of these glucose-regulated transcripts in cells by VFE treatment mean to remarkable glucose responsiveness of the β-cells that might be a key aspects treating diabetes. It has been known that fuel-dependent CREB activation stimulates the expression of pancreatic β-cell-specific genes [29], suggesting that VFE might promote the expression of those genes by glucose-induced CREB activation. Since it was not determined in this study, further investigations are necessary for determining the molecular mechanisms by which VFE regulates gene expression.

2-5. Conclusion

Current study, we proved that the beneficial effects of VFE on insulin sensitivity, thereby relieving metabolic diseases by controlling glucose metabolism with the GSIS. Furthermore, oral VFE administration improved glucose tolerance and insulin sensitivity in peripheral tissues, such as the liver and muscle, which predominate glucose metabolism participation. Although, the mechanism of VFE-stimulated glucose uptake in pancreatic β-cells remains to be elucidated, our findings clearly demonstrate the metabolically beneficial effects of VFE and indicate its potential as a candidate for targeting GSIS to treat T2DM.

2.6 Figures

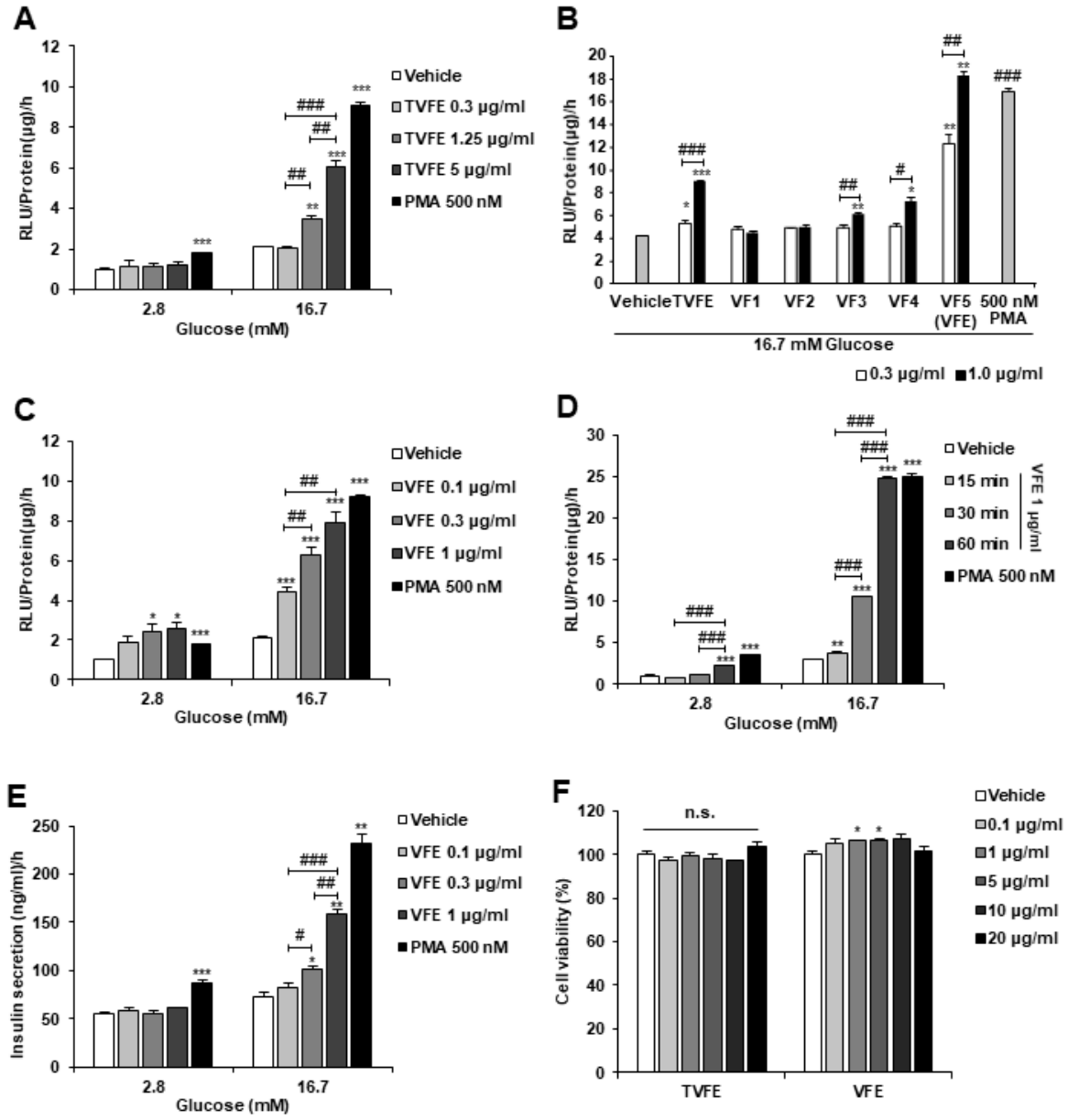

Figure 1. *V. Fordii* extract (VFE) increases insulin secretion in MIN6 cells and Pancreatic islet.

(A) TVFE on insulin release at low (2.8 mM) / high (16.7 mM) glucose dose-dependently in proinsulin-*Gaussia* luciferase-introduced MIN6 cells.

(B) Analysis of insulin secretion from MIN6 cells stimulated with 0.3 and 1 mg/ml of TVFE-subfractions in high glucose condition.

(C) VFE on the insulin release in low and high glucose conditions dose-responsibly in proinsulin-*Gaussia* luciferase-introduced MIN6 cells (n=3).

(D) Time-dependent effect of VFE (1 mg/ml) on luminescent insulin secretion in low / high glucose in MIN6 cells.

(E) The released insulin by VFE in low / high glucose in isolated pancreatic islet dose-dependently.

(F) Dose-response effect of TVFE and VFE for 24 h incubation on MIN6 cell viability.

500 nM PMA was treated to MIN6 cells as a positive control. The luciferase activity was normalized to protein level in each set.

Data are displayed as mean ± S.E.M (n=3). *p<0.05, **p<0.01, ***p<0.001 *vs* vehicle; $^{\#}p$<0.05, $^{\#\#}p$<0.01, $^{\#\#\#}p$<0.001 *vs* each concentration of VFE.

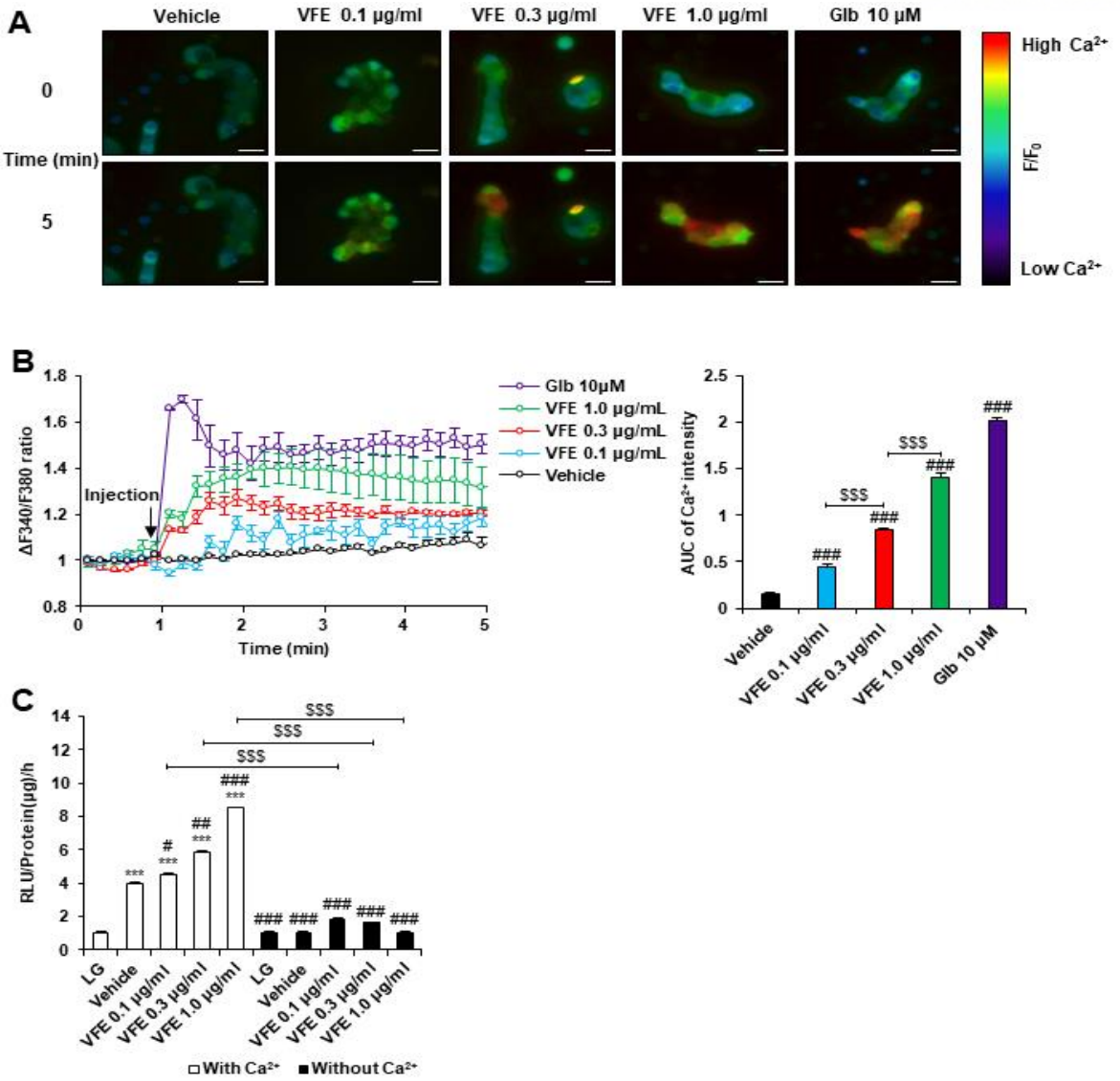

Figure 2. VFE instigated intracellular Ca^{2+} elevation in MIN6 cells.

(A) The representative images visualized VFE-induced intracellular **Ca^{2+}** intensity by Fura-2AM fluorescence ratio (ΔF340/380 nm) in MIN6 cells. The dark and crimson color indicate low and high $[Ca^{2+}]_i$,. Scale bar; 100 μm.

(B) ΔF340/380 nm ratio at the sequential time and the area under curve of ΔF340/380 nm ratio in each concentration of VFE treated MIN6 cells. (n = 5-12 per group).

(C) VFE-stimulated insulin secretion in proinsulin-*Gaussia* luciferase-introduced MIN6 cells in absence or presence of $[Ca^{2+}]_e$ in the high glucose condition. The luciferase intensity was normalized to protein in each set.

Data are presented as mean ± S.E.M (n=3). ***p<0.001 *vs* LG; $^{\#}p$<0.05, $^{\#\#}p$<0.01, $^{\#\#\#}p$<0.001 *vs* vehicle (HG-only); $^{\$\$\$}p$<0.001 *vs* each concentration of VFE.

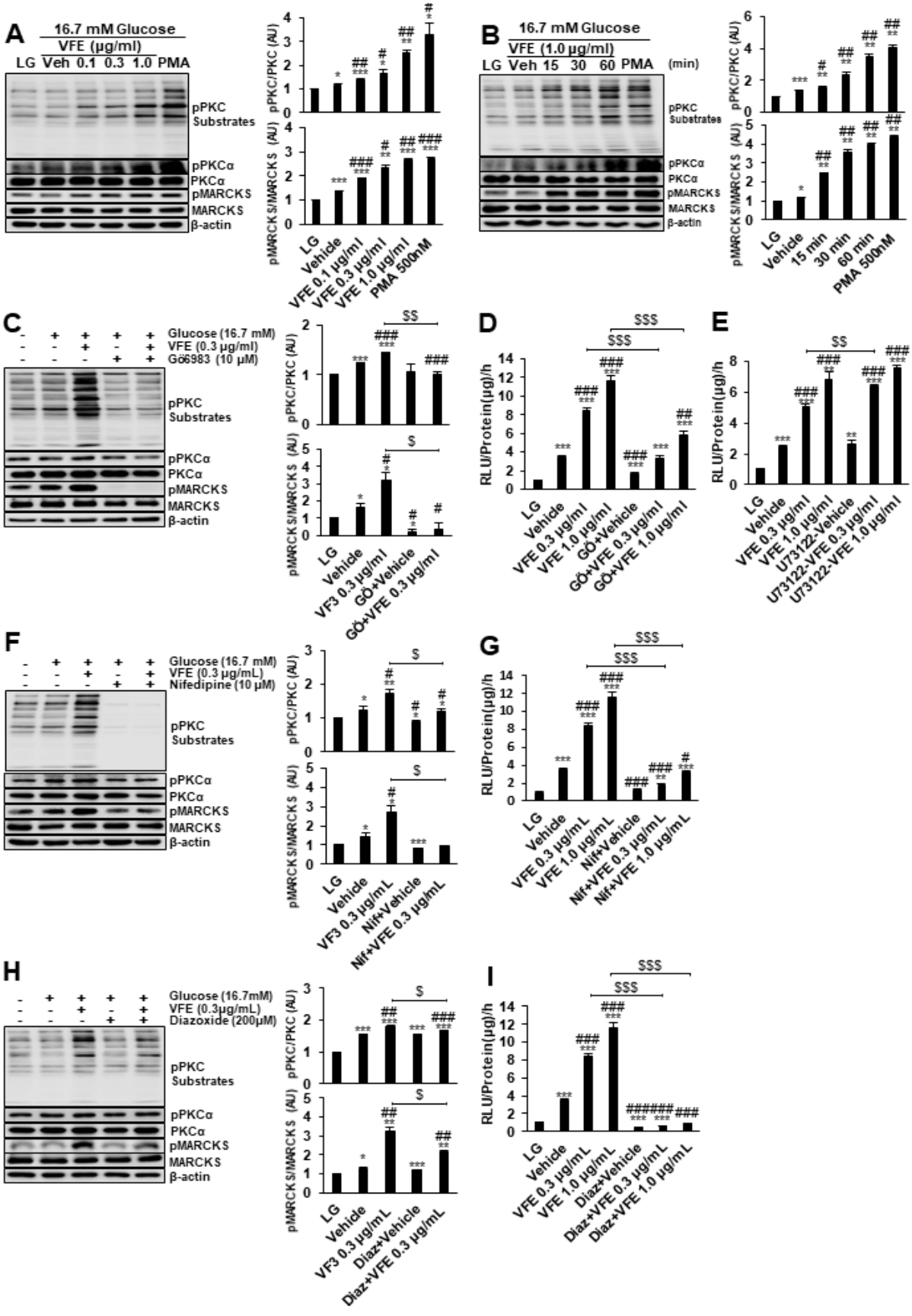

Figure 3. VFE activates PKC and MARCKS in calcium-dependent manner.

(A-B) Western blot assay of pPKC-substrates, PKCα, and MARCKS phosphorylations followed by treatment of MIN6 cells with VFE in dose- **(A)** and time- **(B)** dependent manner.

(C-D) Western blot assay **(C)** and insulin secretion **(D)** followed by treatment of MIN6 cells with VFE at the indicated concentrations alone or together with 10 μM Gö6983 (Gö).

(E) VFE-stimulated insulin secretion was measured in basal or presence with 10 μM U73122 in MIN6 cells.

(F-G) Western blot analysis **(F)** and insulin secretion **(G)** following treatment of MIN6 cells with VFE at the indicated concentrations alone or together with 10 μM nifedipine (Nif).

(H-I) Western blot analysis **(H)** and insulin secretion **(I)** following treatment of MIN6 cells with VFE at the indicated concentrations alone or together with 200 μM diazoxide (Diaz).

The relative pPKCα/PKCα or pMARCKS/MARCKS ratio in all western blot analysis were quantified by ImageJ (AU; arbitrary unit). The luciferase activity was normalized to protein level in each set.

Data are visualized to mean ± S.E.M (n=3). *$p<0.05$, **$p<0.01$, ***$p<0.001$ *vs* LG; $^{\#}p<0.05$, $^{\#\#}p<0.01$, $^{\#\#\#}p<0.001$ *vs* vehicle (HG-only); $^{\$\$}p<0.01$, $^{\$\$\$}p<0.001$ *vs* each concentration of VFE.

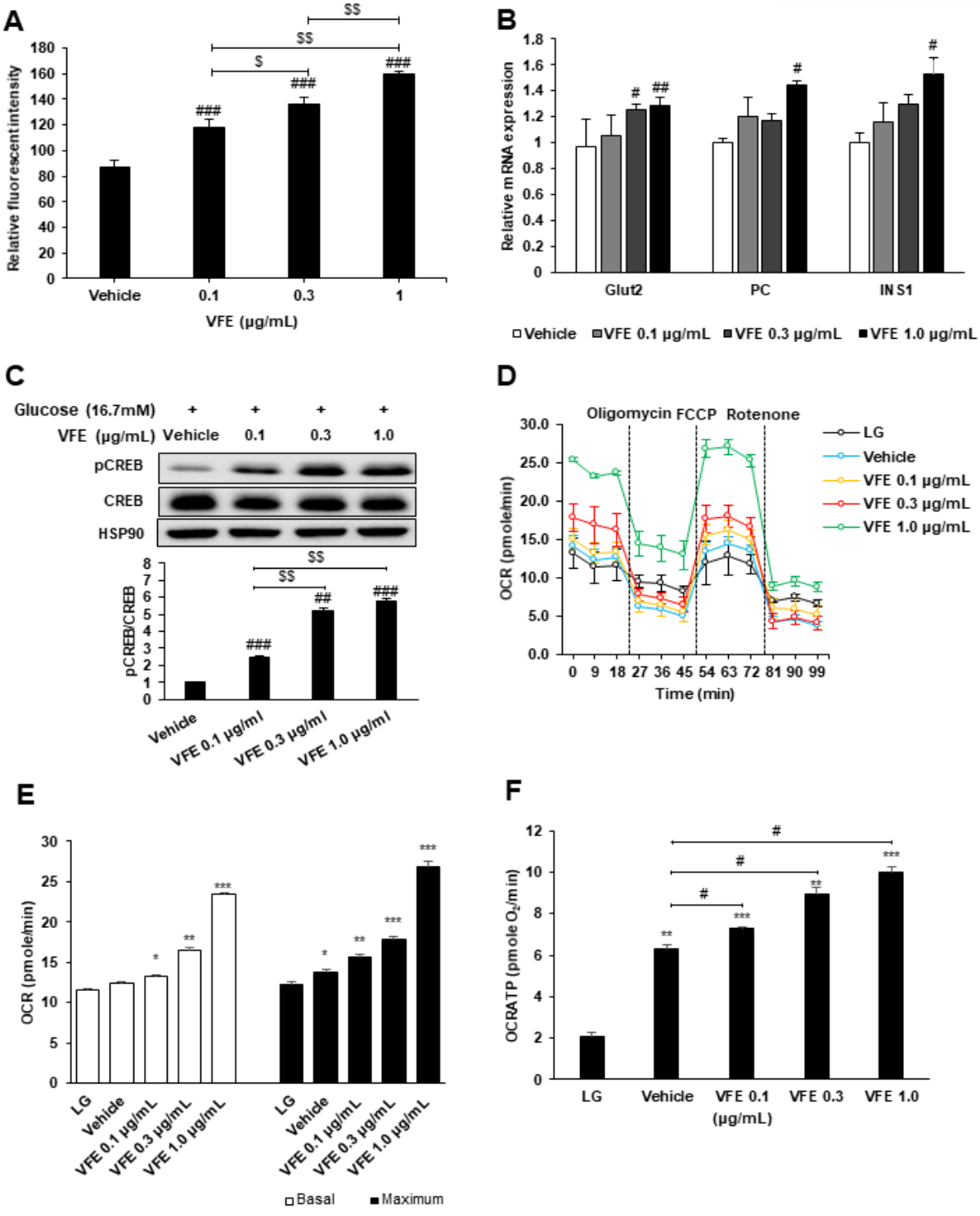

Figure 4. VFE increases glucose uptake and promotes mitochondrial ATP production.

(A) The effect of VFE on glucose uptake in MIN6 cells was measured by 2-NDBG-induced fluorescent intensity.

(B) VFE-treated MIN6 cells were analyzed by qPCR for the gene sets expression (Glut2, PC, and INS1).

(C) Dose-dependent CREB S133 phosphorylation by VFE in MIN6 cells.

(D-F) Oxygen consumption rate **(D)**, Basal/maximum respiration **(E)**, and ATP production **(F)** were measured after treating MIN6 cells with various concentration of VFE as indicated (n=3).

All data are displayed as mean ± S.E.M (n=3). *$p<0.05$, **$p<0.01$, ***$p<0.001$ *vs* LG; $^{\#}p<0.05$, $^{\#\#}p<0.01$, $^{\#\#\#}p<0.001$ *vs* vehicle (HG-only); $^{\$}p<0.05$, $^{\$\$}p<0.01$ *vs* each concentration of VFE.

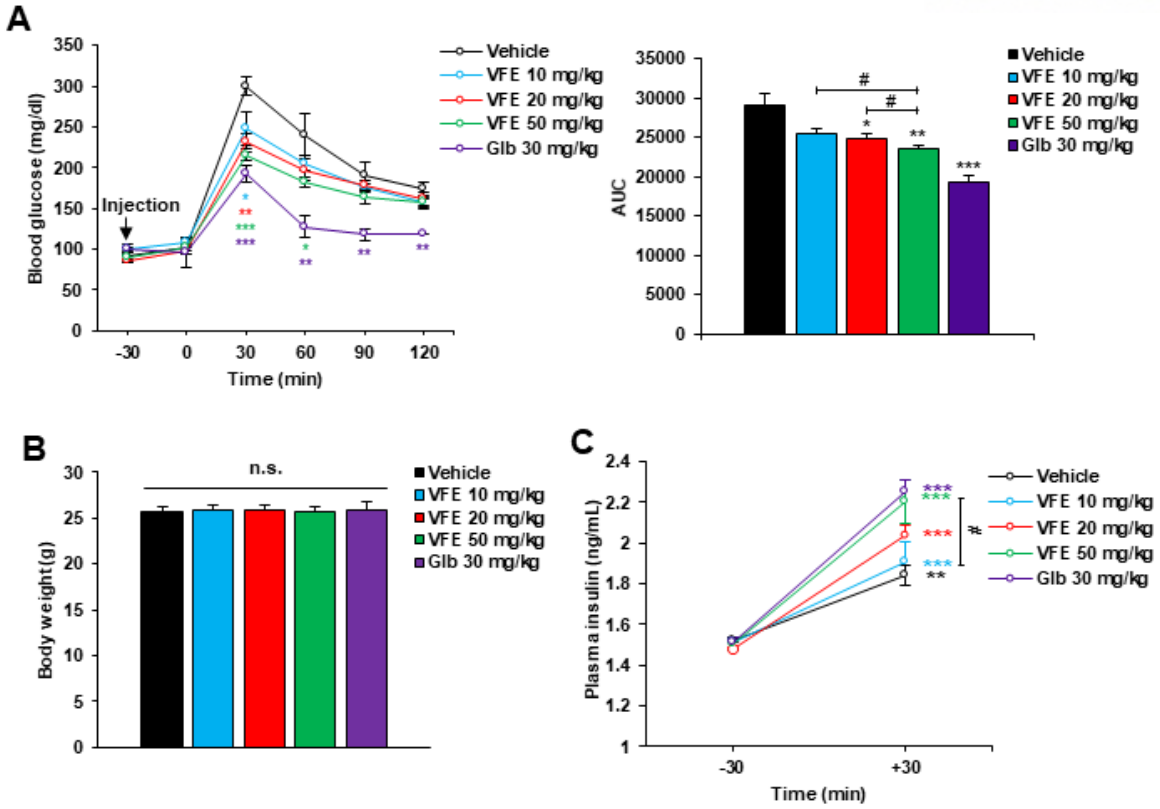

Figure 5. VFE reduces blood glucose in fasted normal mice through increase insulin secretion.

(A-B) Oral GTT test by acute VFE treatment. Right panel, AUC of OGTT **(A)** in NCD-supplied mice with non-weight difference **(B)**. n.s.; not significant. The indicated concentrations of VFE and Glb were orally administrated to mice prior to 30 minutes of 3g/kg glucose oral injection.

(C) Plasma insulin level of VFE or Glb treated NCD-fed mice. -30; the insulin measured in the blood collected before VFE or Glb injection, +30; the insulin measured in the blood collected after 30 min of glucose injection.

Every data is presented as mean ± S.E.M ($n = 5$). *$p < 0.05$, **$p < 0.01$, ***$p < 0.001$ vs group fed vehicle; $^{\#}p < 0.05$ vs each concentration of VFE-treated group.

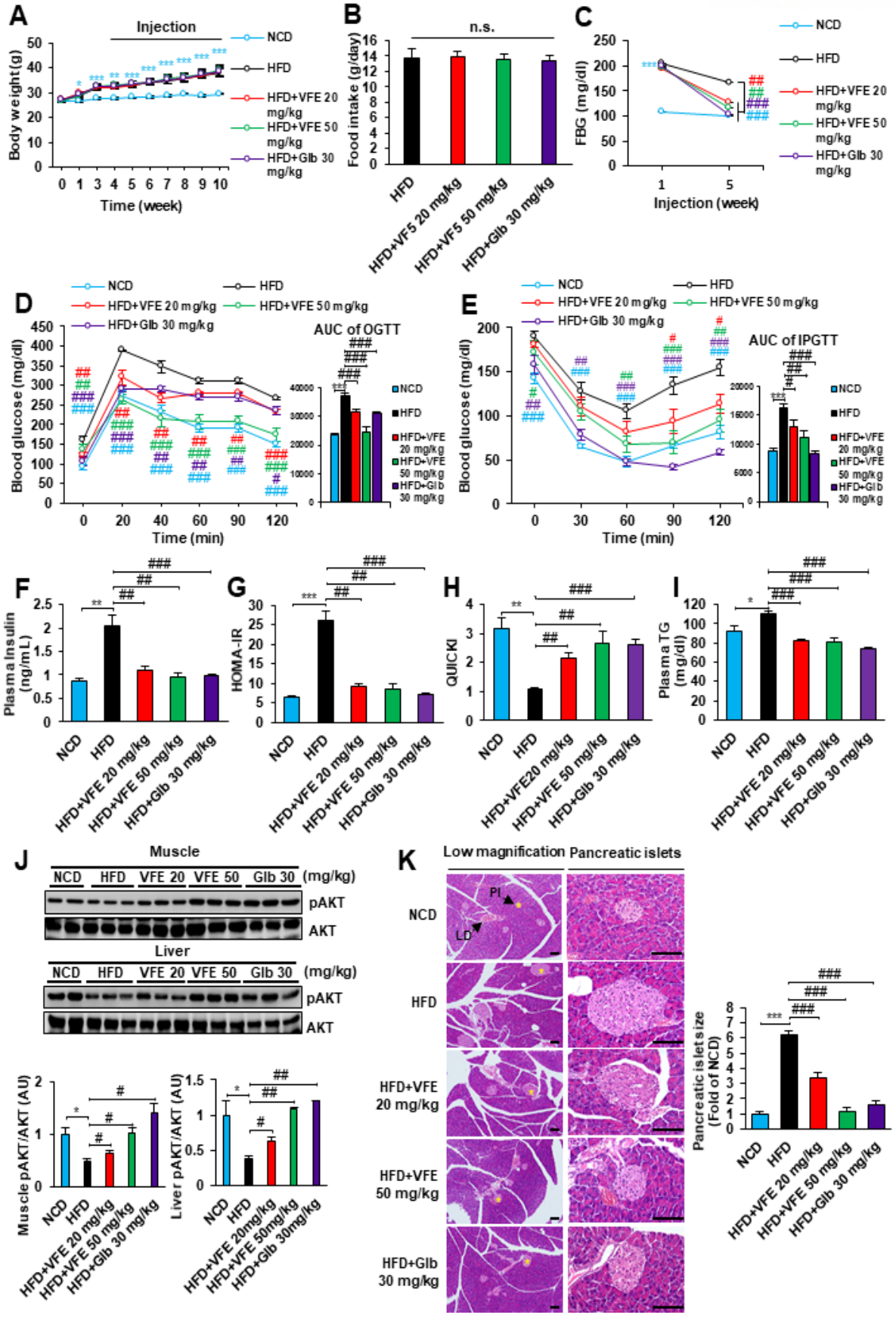

Figure 6. VFE improves insulin sensitivity in diabetic mice.

(A-B) Body weights **(A)** and Food intake **(B)** of HFD-fed mice treated with indicated concentrations of VFE, and Glb or vehicle for 7-weeks. n.s.; not significant.

(C) FBG (fasting blood glucose) level of these mice after 1 week and 5 weeks. OGTT and IPITT were performed in HFD-fed mice treated with vehicle, VFE, and Glb.

(D-E) The blood glucose levels and AUC of OGTT **(D)** and IPITT **(E)** were analyzed.

(F-I) Fasting insulin **(F)**, HOMA-IR **(G)**, QUICKI **(H),** and serum TG **(I)** were measured in these mice.

(J) Activation of Akt (S473 phsophorylation) and total Akt protein in both muscle and liver tissues were analyzed. In western blot analysis, the relative ratio of pAkt/Akt was quantified by ImageJ (AU; arbitrary unit).

(K) Histological images and size of pancreatic islets were performed with Hematoxylin & Eosin (H&E) staining in these mice. The relative fold change of the size of islets compared to NCD-fed mice was quantified by ImageJ. Scale bar; 100 μm. PI; pancreatic islets, LD; intralobular duct.

Entire results are displayed as mean ± S.E.M (n=5). *p<0.05, **p<0.01, ***p<0.001 *vs* NCD-fed group; $^{\#}p$<0.05, $^{\#\#}p$<0.01, $^{\#\#\#}p$<0.001 *vs* HFD-fed group.

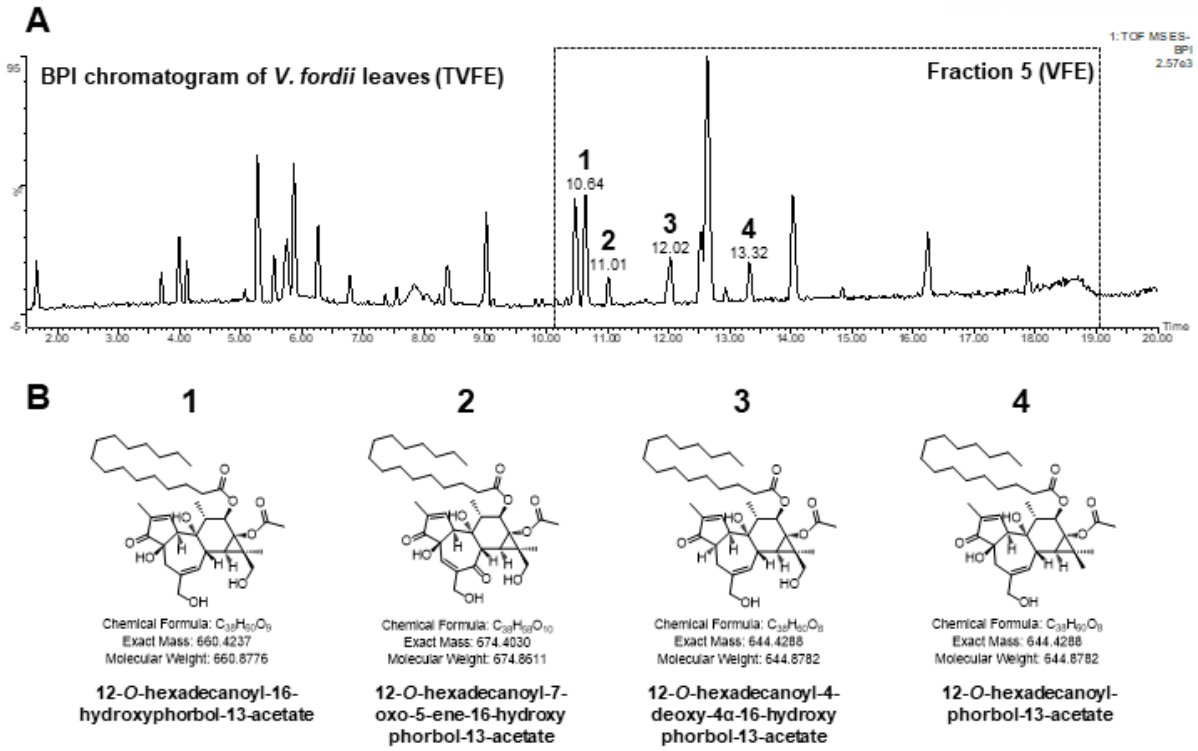

Fig. 7. Analysis of the major constituents of *V. fordii* leaves.

(A) UPLC-QToF-MS chromatograms.

(B) The structure of four tigliane diterpene esters compounds in *V. fordii* leaves.

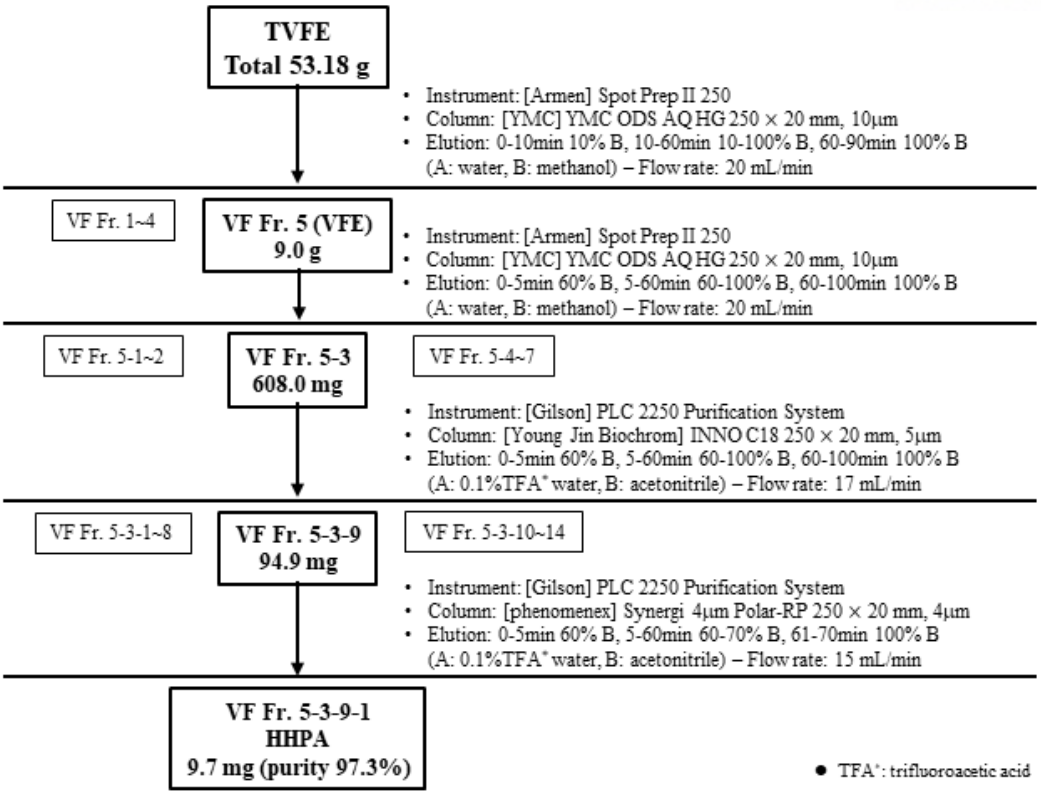

Figure 8. The purification of 12-*O*-hexadecanoyl-16-hydroxyphorbol-13-acetate (HHPA) starting *Vernicia fordii* (Hemsl.) Airy. leaves methanol extract (TVFE)

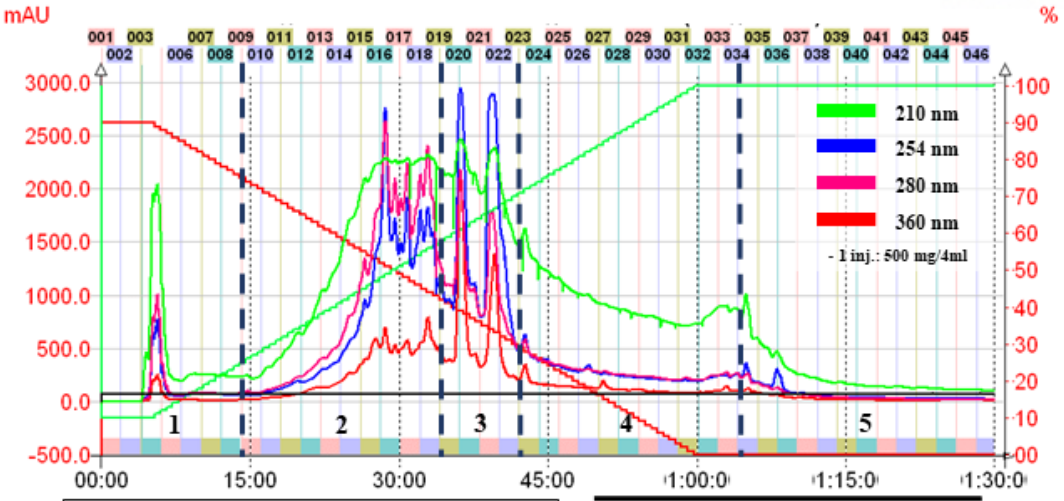

[Armen] Spot Prep II 250
1. Column: YMC ODS AQ HG 220g 250×200 mm, 10 µm
2. Sample: TVFE (53.18 g) - 1 inj.: 500 mg/4ml
3. Method

Time (min)	Flow (mL/min)	%A (water)	%B (methanol)
(Initial)	20.0	95	10
15.00	20.0	95	10
65.00	20.0	70	100
90.00	20.0	0	100

Fraction	Weight (g)
VFL Fr. 1	19.6
VFL Fr. 2	11.9
VFL Fr. 3	6.5
VFL Fr. 4	3.3
VFL Fr. 5 (VFE)	9.0

Figure 9. The MPLC chromatogram of TVFE.

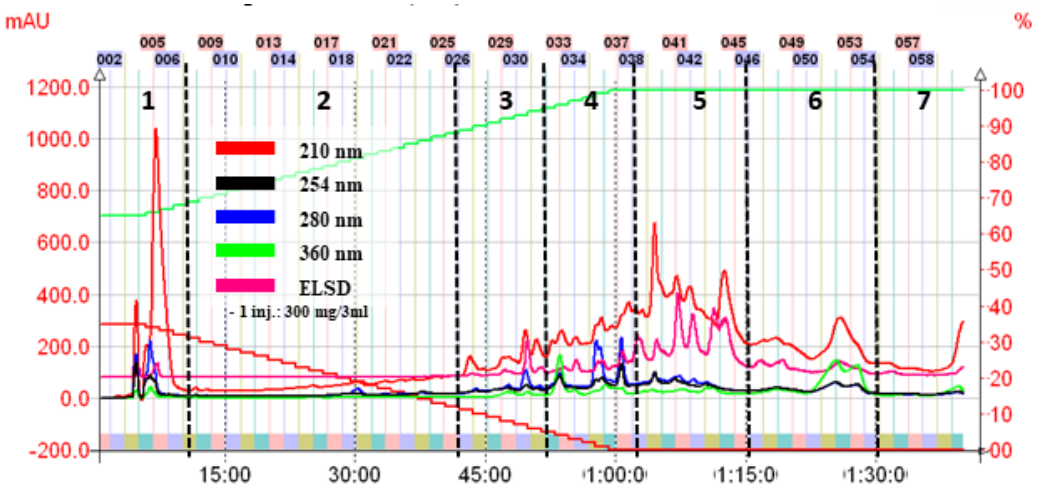

[Armen] Spot Prep II 250
1. Column: YMC ODS AQ HG 220g 250×200 mm, 10 µm
2. Sample: VF Fr. 5 (9.0 g) - 1 inj.: 500 mg/4ml
3. Method

Time (min)	Flow (mL/min)	%A (water)	%B (methanol)
(Initial)	20.0	95	60
5.0	20.0	95	60
60.0	20.0	70	100
100.0	20.0	0	100

Fraction	Weight (mg)	Fraction	Weight (mg)
VFL Fr. 5-1	306.2	VFL Fr. 5-5	681.7
VFL Fr. 5-2	286.8	VFL Fr. 5-6	444.3
VFL Fr. 5-3	608.8	VFL Fr. 5-7	291.8
VFL Fr. 5-4	842.6		

Figure 10. The MPLC chromatogram of VF Fr. 5 (VFE).

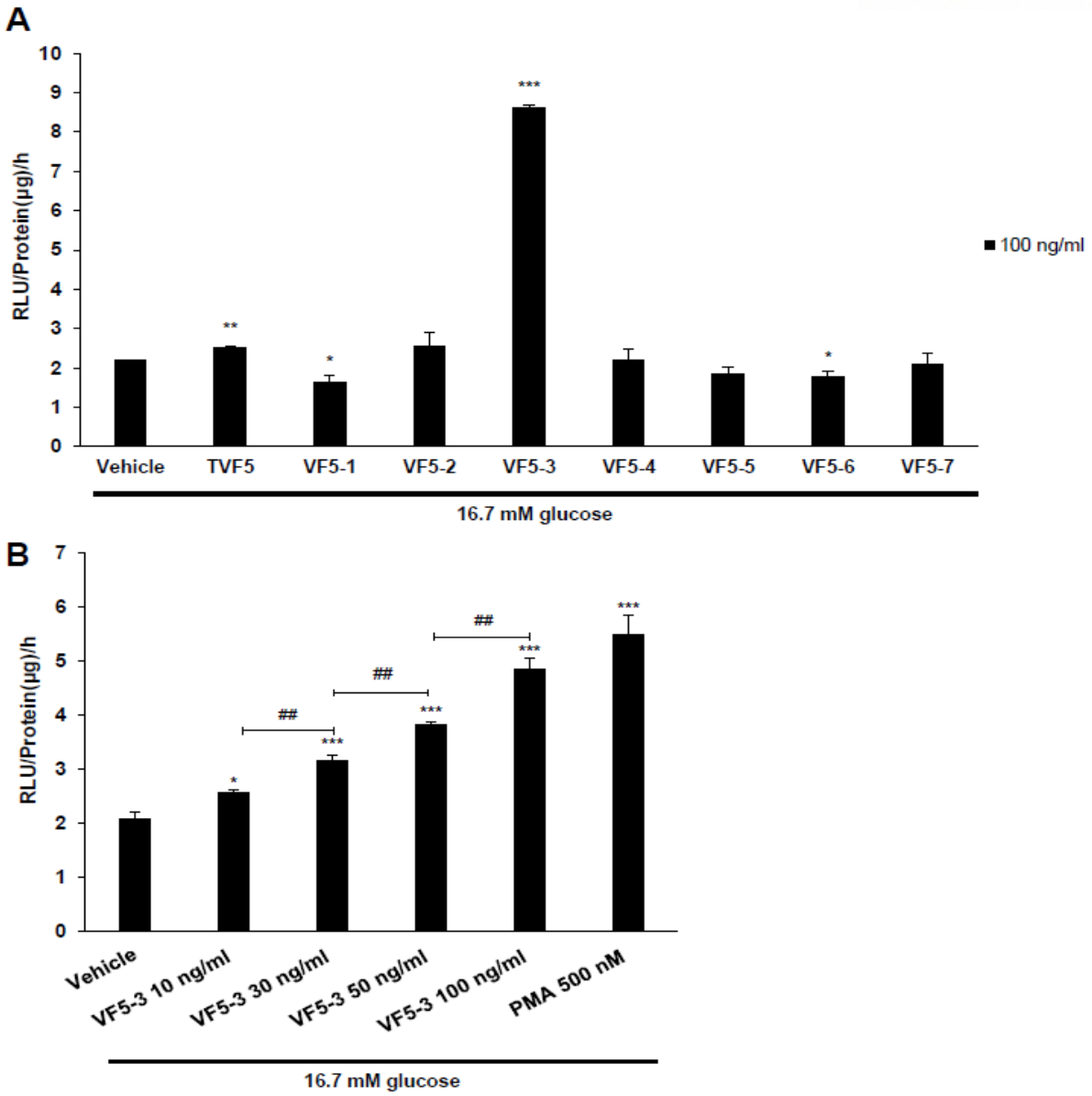

Figure 11. The MPLC fractions of VFE screening to confirm increased insulin release in MIN6 cells.

(A) Analysis of insulin secretion stimulated by the 100 ng/ml VF Fr.5-derived fractions in high glucose condition (n=3).

(B) Measurement of insulin secretion stimulated with the 10, 30, 50, and 100 ng/ml VF5-3 in high glucose condition (n=3).

All research data are displayed as mean ± S.E.M. *p<0.05, **p<0.01, ***p<0.001 vs Vehicle; $^{\#\#}p$<0.01 vs each concentration of VF Fr.5.

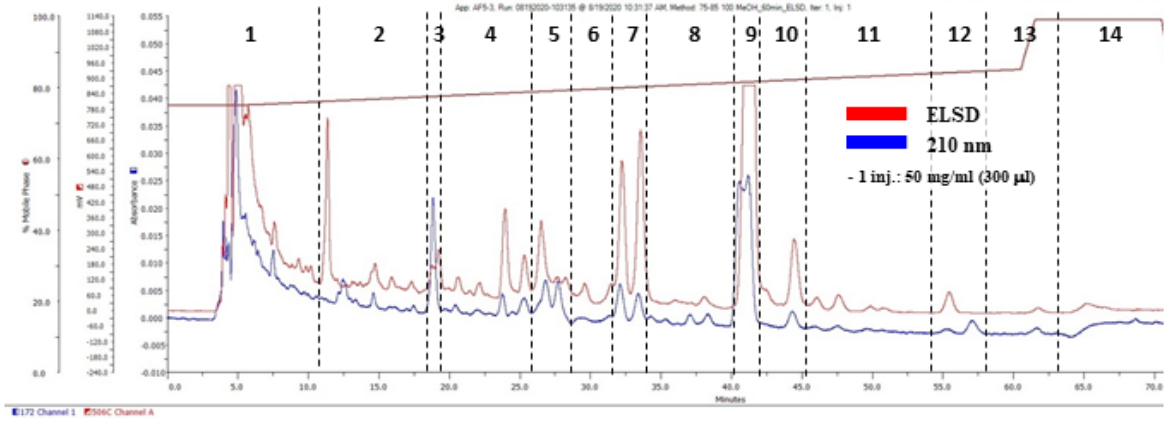

[Gilson] PLC 2250 Purification System
1. Column: INNO C18 250×200 mm, 5 µm
2. Sample: VFL Fr. 5-3 (608.0 mg) - 1 inj.: 50 mg/ml (300 µl)
3. Method

Time (min)	Flow (mL/min)	%A (0.1% TFA water)	%B (acetonitrile)
(Initial)	10	25	75
5.00	17	25	75
60.00	17	15	85
61.00	17	0	100
70.00	17	0	100

Fraction	Weight (mg)	Fraction	Weight (mg)
VFL Fr.5-3-1	372.8	VFL Fr.5-3-8	151.9
VFL Fr.5-3-2	334.3	VFL Fr.5-3-9	94.9
VFL Fr.5-3-3	52.6	VFL Fr.5-3-10	70.4
VFL Fr.5-3-4	208.8	VFL Fr.5-3-11	183.5
VFL Fr.5-3-5	81.8	VFL Fr.5-3-12	64.0
VFL Fr.5-3-6	81.5	VFL Fr.5-3-13	62.7
VFL Fr.5-3-7	84.7	VFL Fr.5-3-14	101.3

Figure 12. The prep-HPLC chromatogram of VF Fr. 5-3

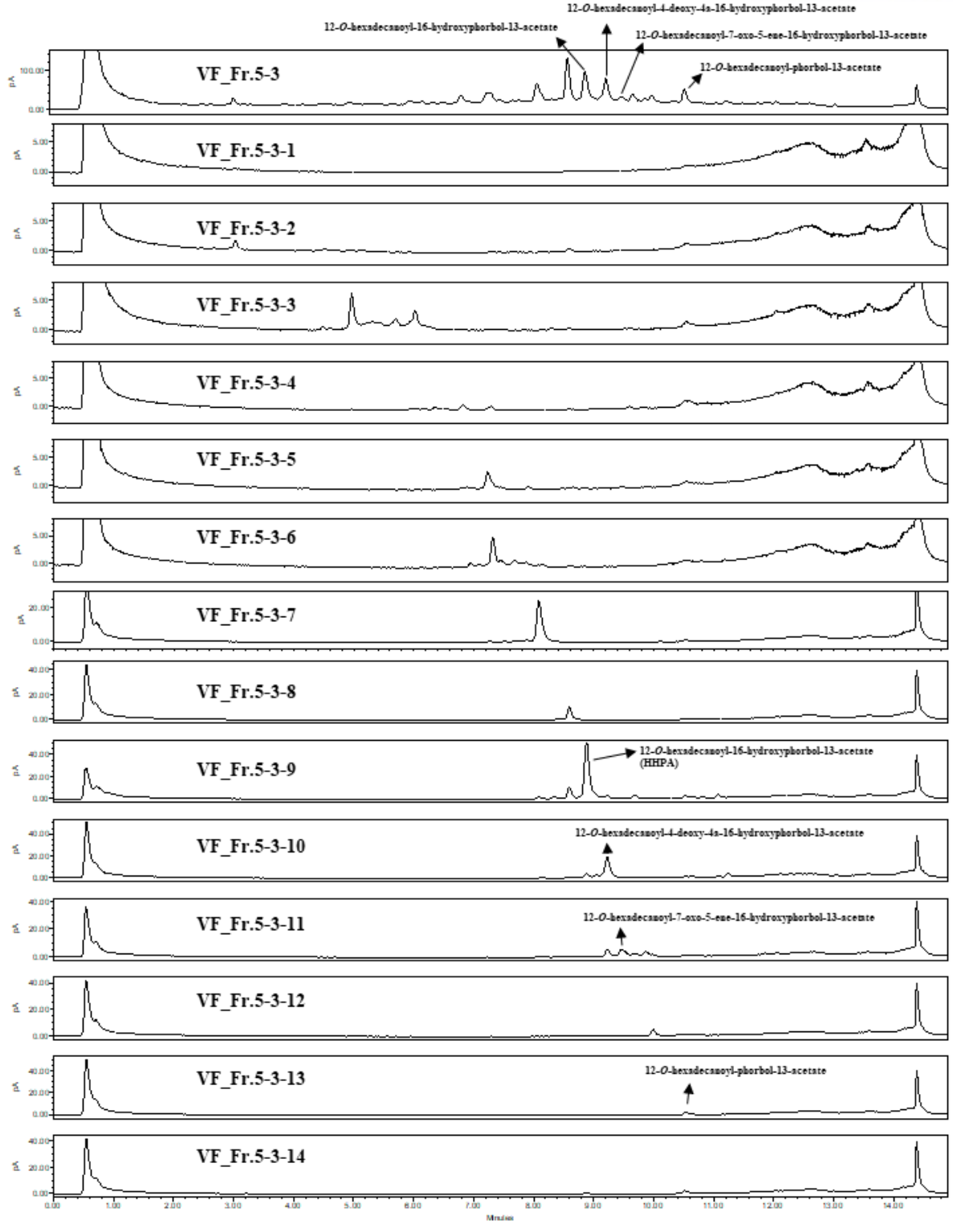

Figure 13. The CAD Chromatogram of VF Fr.5-3 subtraction.

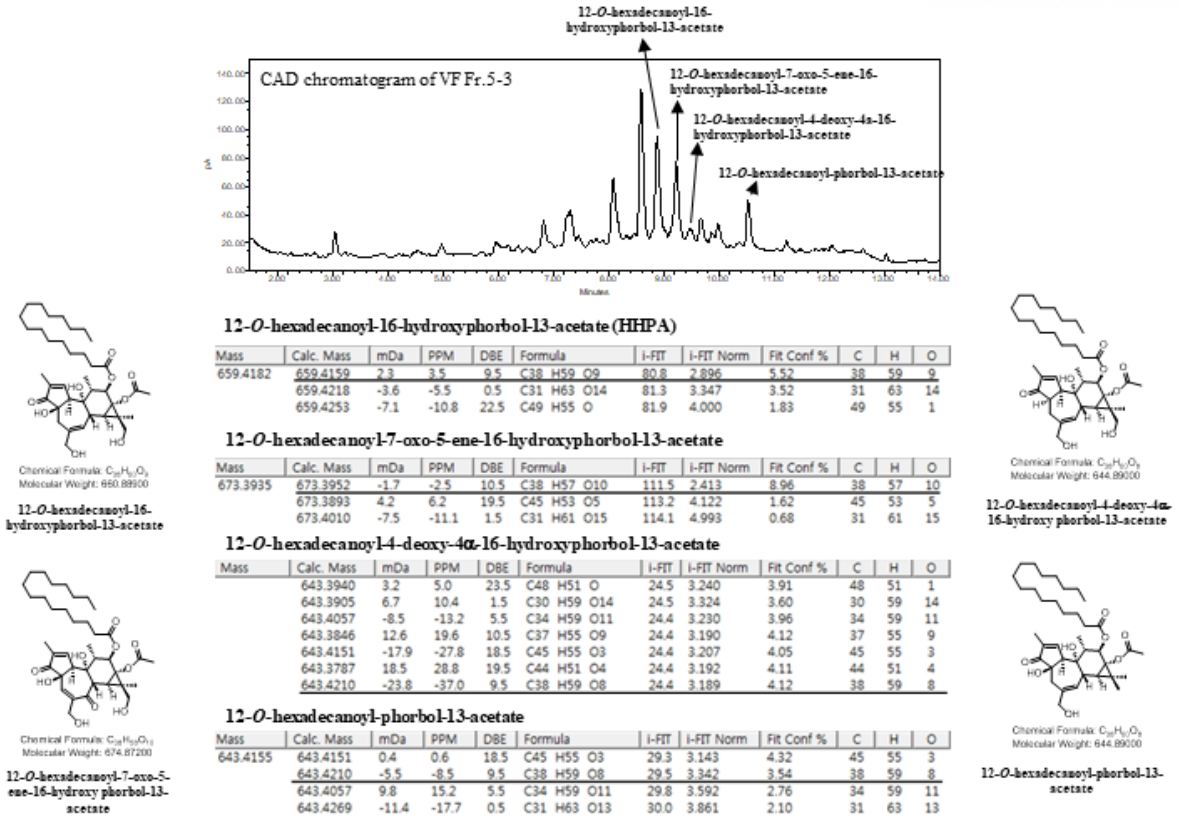

Figure 14. HRMS of four tigliane-type diterpene esters in VF Fr.5-3

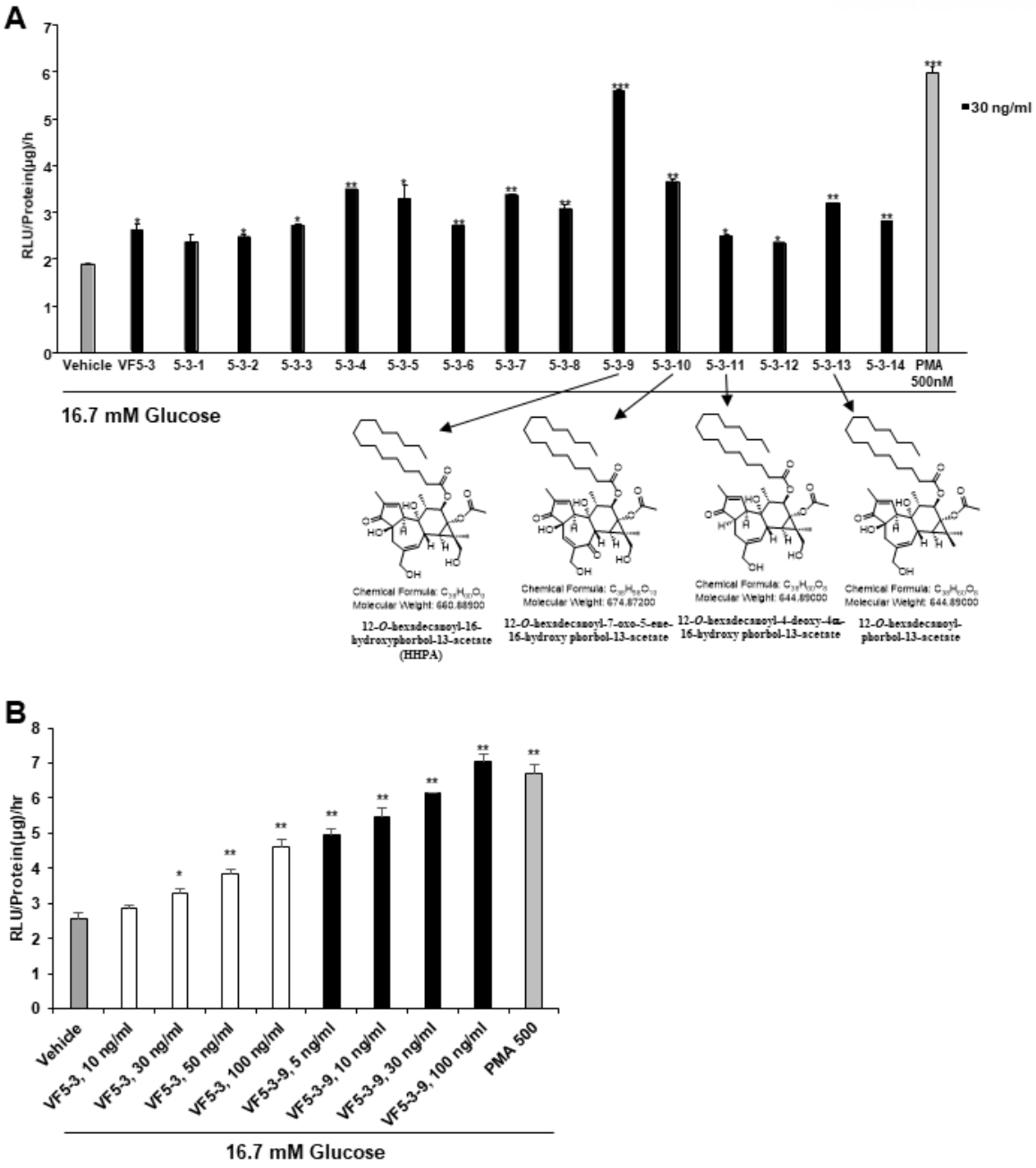

Figure 15. VF Fr. 5-3 subfractions screening to confirm increased insulin release in MIN6 cells.

(A) Analysis of insulin secretion stimulated by the 30 ng/ml VF Fr.5-3-derived fractions in 16.7 mM glucose condition in MIN6 cells (n=3).

(B) Analysis of insulin secretion stimulated by the indicated concentrations of VF5-3 and VF5-3-9 in 16.7 mM glucose condition in MIN6 cells (n=3).

Entire results are displayed as mean ± S.E.M. *p<0.05, **p<0.01, ***p<0.001 vs Vehicle.

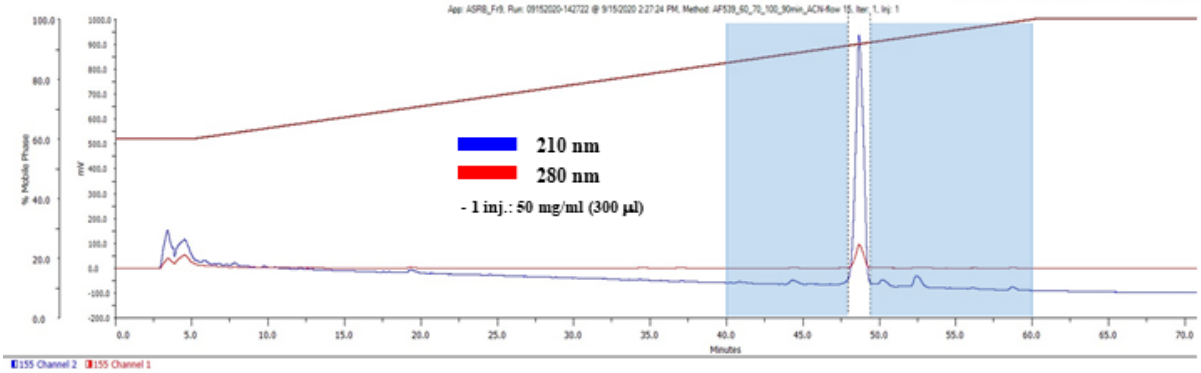

[Gilson] PLC 2250 Purification System
1. Column: Synergi 4mm Polar-RP 250 × 20 mm, 4µm
2. Sample: VFL Fr. 5-3-9 (94.9 mg)
- 1 inj.: 50 mg/ml (300 µl)
3. Method

Time (min)	Flow (mL/min)	%A (0.1% TFA water)	%B (acetonitrile)
(Initial)	10	25	60
5.00	15	25	60
60.00	15	15	70
61.00	15	0	100
70.00	15	0	100

Fraction	Weight(mg)
VFL Fr. 5-3-9-1	9.7

Figure 16. The prep-HPLC chromatogram of VF Fr. 5-3-9

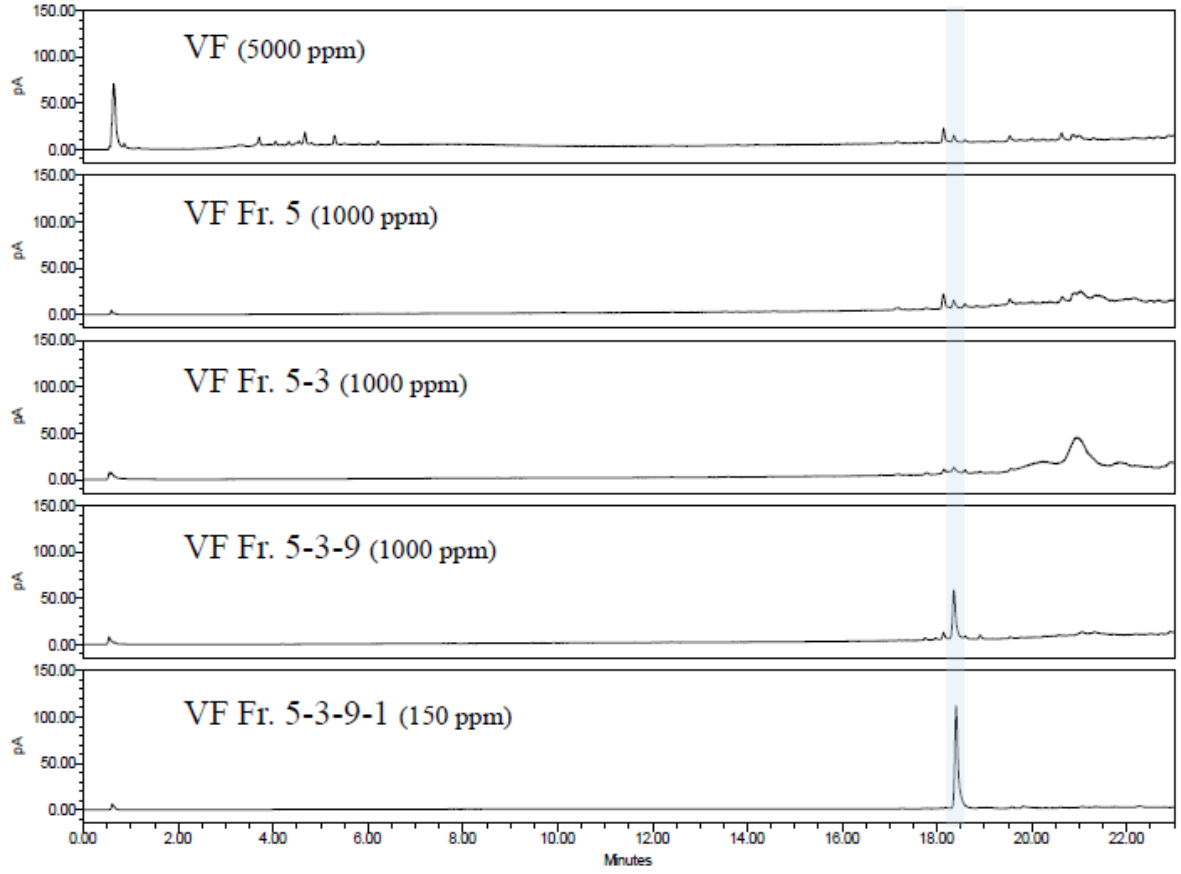

Figure 17. The UPLC chromatogram of isolated HHPA.

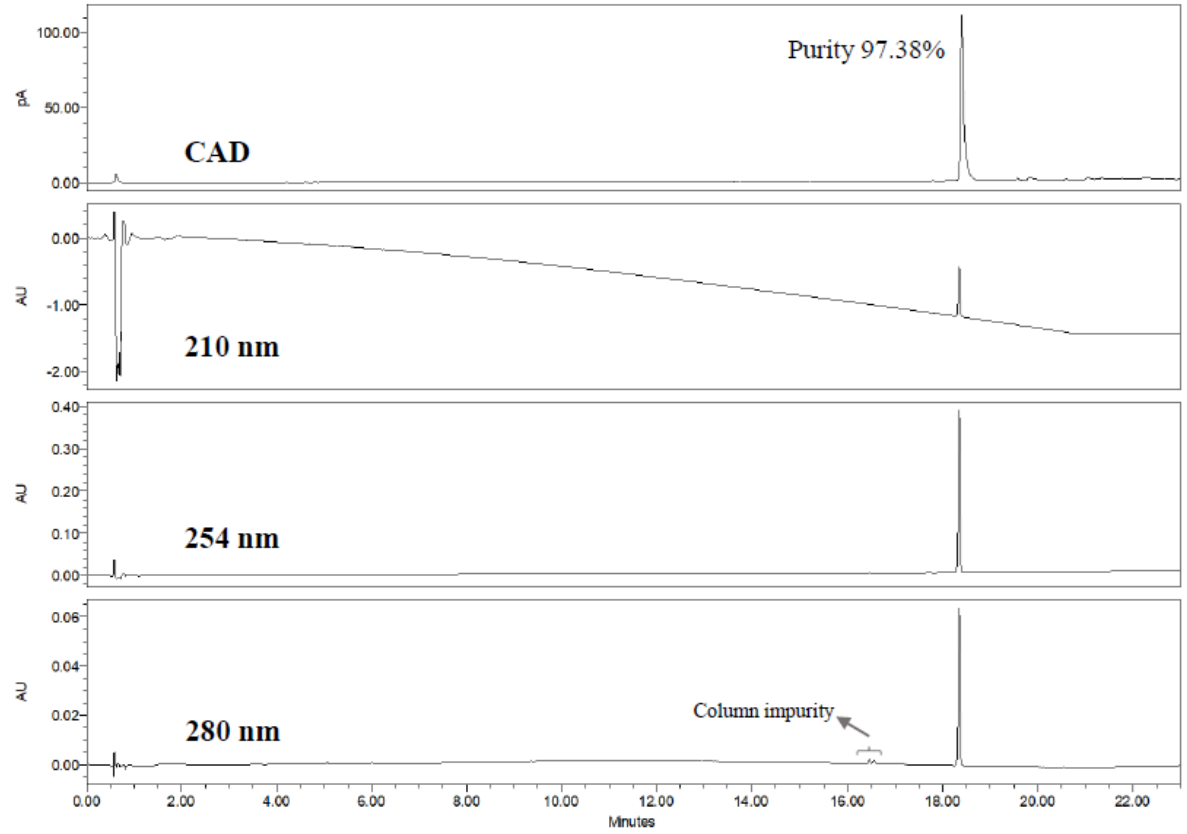

Figure 18. The UPLC chromatogram of VF Fr. 5-3-9-1 to determine the purity of isolated HHPA.

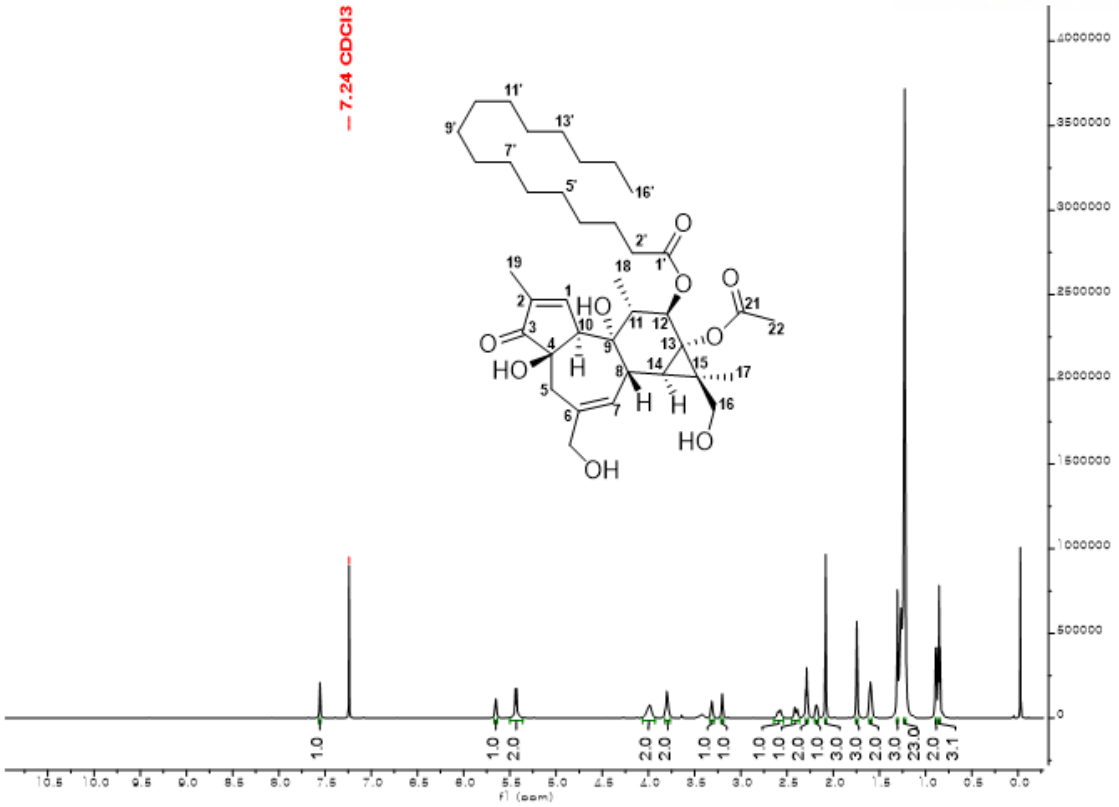

Figure 19. ^{1}H NMR spectrum of HHPA (700 MHz, chloroform-*d*).

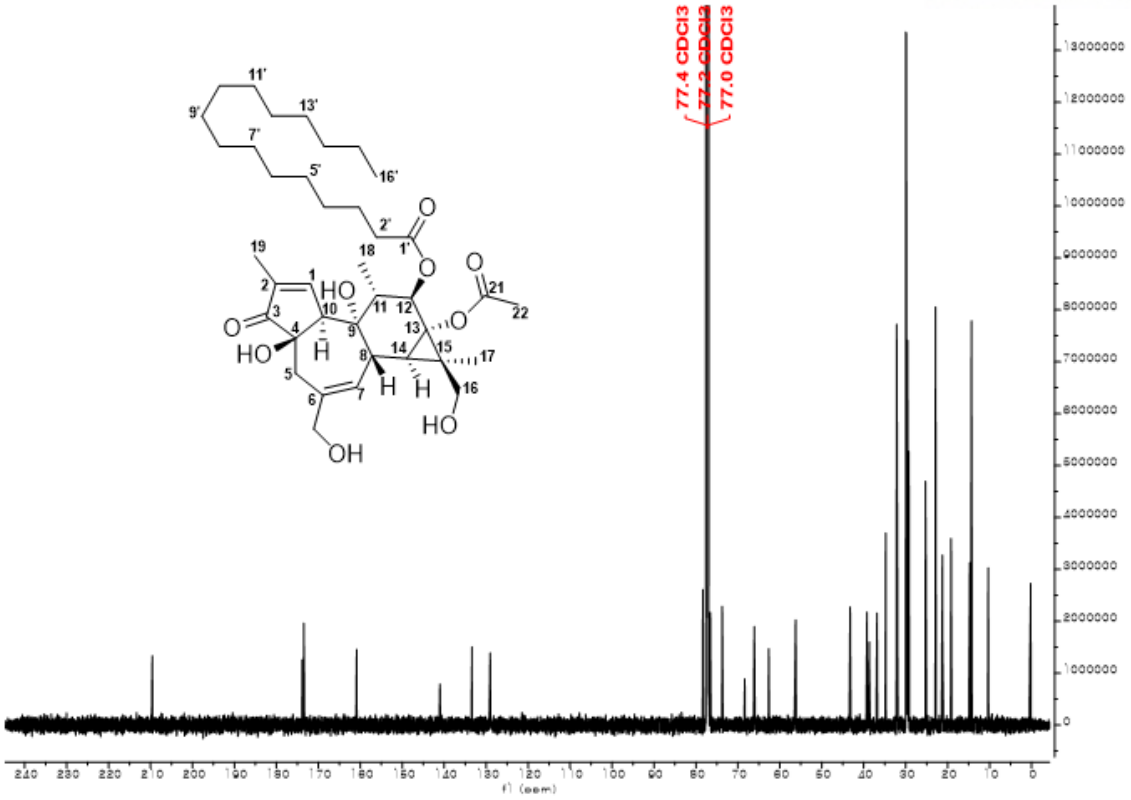

Figure 20. ^{13}C NMR spectrum of HHPA (175 MHz, chloroform-*d*).

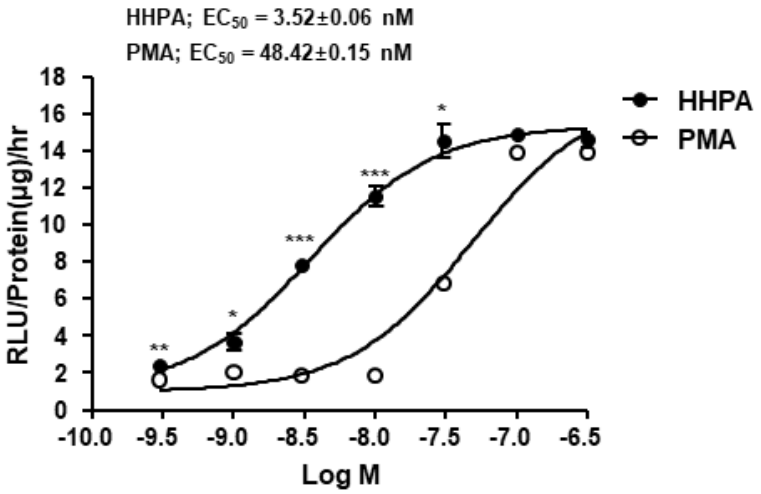

Figure 21. Insulinotrophic effect of HHPA from VFE in MIN6 cells. *p<0.05, **p<0.01, ***p<0.001 vs matched concentration of PMA.

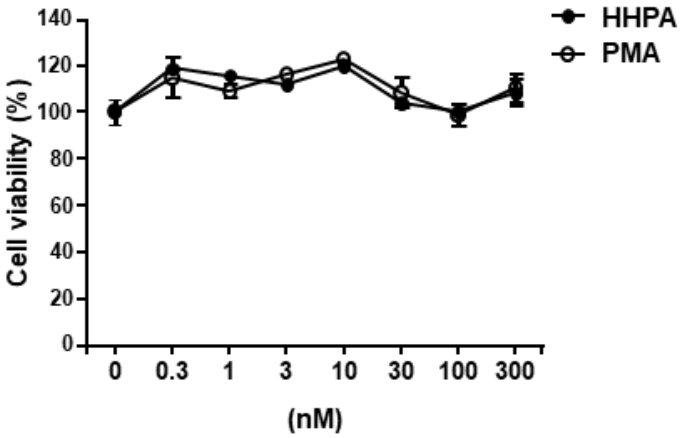

Figure 22. Cytotoxicity of HHPA from VFE in MIN6 cells.

2-7 Tables

	Compounds	Retention time [min]	UV (nm)	Detected ion $[M-H]^-$	Calculated ion $[M-H]^-$	MS fragments	Error (ppm)	Molecular formula
1	12-*O*-hexadecanoyl-16-hydroxyphorbol-13-acetate	10.64	231	659.4182	659.4159	255	3.5	$C_{38}H_{60}O_9$
2	12-*O*-hexadecanoyl-7-oxo-5-ene-16-hydroxyphorbol-13-acetate	11.01	227	673.3935	673.3952	357, 339, 327	-2.5	$C_{38}H_{58}O_{10}$
3	12-*O*-hexadecanoyl-4-deoxy-4a-16-hydroxyphorbol-13-acetate	12.02	232	643.4205	643.4210	325, 307, 255	-0.8	$C_{38}H_{60}O_8$
4	12-*O*-hexadecanoyl-phorbol-13-acetate	13.32	227	643.4155	643.4210	313, 255	-8.5	$C_{38}H_{60}O_8$

Table 1. The UV, m/z values, MS fragments, and molecular formulae in negative ion mode for peak assignments of compounds (1-4) by UPLC-QToF-MS in *V. fordii* leaves.

Position	VFL Fr. 5-3-9-1 (HHPA)		Published spectroscopic data*		Position	VFL Fr. 5-3-9-1 (HHPA)		Published spectroscopic data*	
	^{1}H (d_H)	^{13}C (d_C)	^{1}H (d_H)	^{13}C (d_C)		^{1}H (d_H)	^{13}C (d_C)	^{1}H (d_H)	^{13}C (d_C)
1	7.56 (1H, s)	160.9	7.56, broad s	160.5	palmitoyl				
2		141.0		140.8	1'		173.5		173.3
3		209.6		209.4	2'	2.28 (2H, br t, J = 7.2 Hz)	34.8	2.29, t	34.5
4		73.7		73.5	3'	1.60 (2H, m)	25.3	1.24, s	25.1
5	2.39 (1H, d, *J* = 18.0 Hz) 2.58 (1H, d, *J* = 18.0 Hz)	38.7	obscured	38.1	4'	1.23 (23H, overlap)	29.2	1.24, s	29.0
					5'	1.23 (23H, overlap)	29.5	1.24, s	29.3
6		133.4		133.1	6'-13'	1.23 (23H, overlap)	29.6-29.9	1.24, s	29.7
7	5.65 (1H, s)	129.0	5.64, m	128.8	14'	1.23 (23H, overlap)	32.1	1.24, s	31.9
8	3.31 (1H, s)	56.2	3.36, m	55.9	15'	1.27 (2H, overlap)	22.9	1.24, s	22.7
					16'	0.85 (3H, t, J = 6.86 Hz)	14.3	0.86, t	14.1
9		78.4		78.3					
10	3.20 (1H, s)	43.2	3.20, m	42.9					
11	2.18 (1H, t, *J* = 8.7 Hz)	39.2	ca. 2.18	39.1					
12	5.43 (2H, d, *J* = 10.0 Hz)	76.6	5.41, d	76.4					
13		66.1		65.9					
14	1.23 (23H, overlap)	36.8	1.23, m	36.5					
15		31.9		31.8					
16	3.80 (2H, br t)	62.6	3.80, s	62.0					
17	1.30 (3H, s)	19.2	1.30, s	14.6					
18	0.88 (2H, d, J = 5.9 Hz)	14.7	0.88, d	10.1					
19	1.75 (3H, s)	10.3	1.73, m	18.8					
20	3.98 (2H, br t)	68.4	3.97, s	67.9					
21		173.8		173.6					
22	2.08 (3H, s)	21.2	2.08, s	21.0					

* ref.: Hirota, M., Ohigash, H., Koshimizu K., 1979. Piscicidal Constituents and Related Diterpene Esters from *Aleurites fordii*. Agric. Biol. Chem. 43 (12), 2523-2529.

Table 2. The comparison of the ^{1}H (700 MHz) and ^{13}C (175 MHz) data of HHPA and published spectroscopic data

	VFL Fr.5391-1		VFL Fr.5391-2		VFL Fr.5391-3		Average	
	ppm	area	ppm	area	ppm	area	ppm	area
VFL Fr.5391	1	2386663	1	2100932	1	1940549	1	2142714.667
	5	11424407	5	10781408	5	12468296	5	11558037
	10	24172692	10	22316866	10	21808196	10	22765918
	25	52251756	25	53610604	25	56480386	25	54114248.67
	50	100707722	50	100666796	50	103266382	50	101546966.7
	60	120771601	60	120975991	60	119428362	60	120391984.7
	75	150935859	75	153123213	75	149751528	75	151270200
Slope	1983306.198		2013485.787		1976523.539		1991105.175	
Intercept	2060499.888		1218288.863		2635625.59		1971471.447	
							LOD	3.26746
							LOQ	9.901393

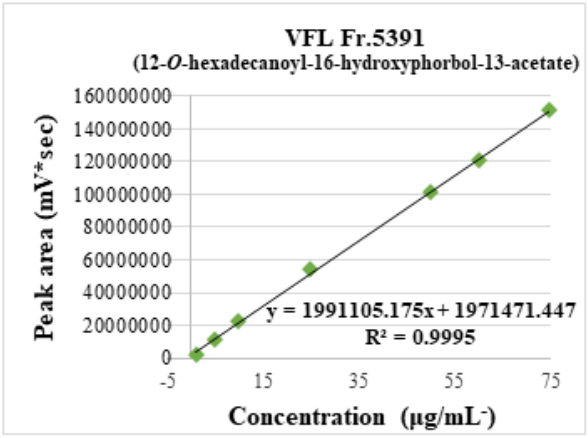

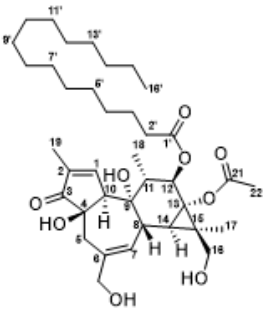

Table 3. Calibration curve of HHPA (12-*O*-hexadecanoyl-16-hydroxyphorbol-13-acetate)

Name	Sequence (5'→3')
Real-time PCR (F- Forward primer; R- Reverse primer)	
Glut2 (F)	CCGAACTGGAAGGAACTCAG
Glut2 (R)	GGATTAAGCGGACAATTCCA
Pyruvate carboxylase (F)	GGGATGCCCACCAGTCACT
Pyruvate carboxylase (R)	CATAGGGCGCAATCTTTTTGA
Ins1 (F)	ATCAGAGACCATCAGCAAGC
Ins1 (R)	GTTTGACAAAAGCCTGGGTG
Rpl32 (F)	CAATGTGTCCTCTAAGAACCGAAA
Rpl32 (R)	CCTGGCGTTGGGATTGG

Table 4. List of primer sequences for the real-time PCR

Name	Abbreviation	role
Diazoxide	Diaz	K_{ATP} channel opener
Nifedipine	Nif	L–VDCC inhibitor
GÖ6983	GÖ	PKC inhibitor
U73122	U73122	PLC inhibitor

Table 5. List of inhibitors for GSIS used in this thesis

2-8. Reference

1. DeFronzo, R. A.; Ferrannini, E.; Groop, L.; Henry, R. R.; Herman, W. H.; Holst, J. J.; Hu, F. B.; Kahn, C. R.; Raz, I.; Shulman, G. I.; Simonson, D. C.; Testa, M. A.; Weiss, R., Type 2 diabetes mellitus. *Nat Rev Dis Primers* **2015,** *1*, 15019.

2. LeRoith, D., Beta-cell dysfunction and insulin resistance in type 2 diabetes: role of metabolic and genetic abnormalities. *Am J Med* **2002,** *113 Suppl 6A*, 3s-11s.

3. Stumvoll, M.; Goldstein, B. J.; van Haeften, T. W., Type 2 diabetes: principles of pathogenesis and therapy. *Lancet* **2005,** *365* (9467), 1333-46.

4. Dias, D. A.; Urban, S.; Roessner, U., A historical overview of natural products in drug discovery. *Metabolites* **2012,** *2* (2), 303-336.

5. Kingston, D. G., Modern natural products drug discovery and its relevance to biodiversity conservation. *Journal of natural products* **2011,** *74* (3), 496-511.

6. Singh, J.; Cumming, E.; Manoharan, G.; Kalasz, H.; Adeghate, E., Suppl 2: Medicinal chemistry of the anti-diabetic effects of Momordica charantia: active constituents and modes of actions. *The open medicinal chemistry journal* **2011,** *5*, 70.

7. Burns, Sean M.; Vetere, A.; Walpita, D.; Dančík, V.; Khodier, C.; Perez, J.; Clemons, Paul A.; Wagner, Bridget K.; Altshuler, D., High-Throughput Luminescent Reporter of Insulin Secretion for Discovering Regulators of Pancreatic Beta-Cell Function. *Cell Metabolism* **2015,** *21* (1), 126-137.

8. Association, A. D., Diagnosis and Classification of Diabetes Mellitus. *Diabetes Care* **2005,** *28* (1), S37.

9. Weyer, C.; Bogardus, C.; Mott, D. M.; Pratley, R. E., The natural history of insulin secretory dysfunction and insulin resistance in the pathogenesis of type 2 diabetes mellitus. *The Journal of clinical investigation* **1999,** *104* (6), 787-794.

10. Jensen, T.; Deckert, T., Diabetic retinopathy, nephropathy and neuropathy. Generalized vascular damage in insulin-dependent diabetic patients. *Horm Metab Res Suppl* **1992,** *26*, 68-70.

11. Azoulay, L.; Suissa, S., Sulfonylureas and the Risks of Cardiovascular Events and Death: A Methodological Meta-Regression Analysis of the Observational Studies. *Diabetes Care* **2017,** *40* (5), 706-714.

12. Straub, S. G.; Sharp, G. W., Glucose-stimulated signaling pathways in biphasic insulin secretion. *Diabetes Metab Res Rev* **2002,** *18* (6), 451-63.

13. Yaney, G. C.; Fairbanks, J. M.; Deeney, J. T.; Korchak, H. M.; Tornheim, K.; Corkey, B. E., Potentiation of insulin secretion by phorbol esters is mediated by PKC-α and nPKC isoforms. *American Journal of Physiology-Endocrinology and Metabolism* **2002,** *283* (5), E880-E888.

14. Wan, Q.-F.; Dong, Y.; Yang, H.; Lou, X.; Ding, J.; Xu, T., Protein kinase activation increases insulin secretion by sensitizing the secretory machinery to Ca2+. *The Journal of general physiology* **2004,** *124* (6), 653-662.

15. Katiyar, C.; Gupta, A.; Kanjilal, S.; Katiyar, S., Drug discovery from plant sources: An integrated approach. *AYU (An international quarterly journal of research in Ayurveda)* **2012,** *33* (1), 10-19.

16. Zheng, J.; Zhao, Y.; Lun, Q.; Song, Y.; Shi, S.; Gu, X.; Pan, B.; Qu, C.; Li, J.; Tu, P., Corydalis

edulis Maxim. promotes insulin secretion via the activation of protein kinase Cs (PKCs) in mice and pancreatic β cells. *Scientific reports* **2017,** *7* (1), 1-11.

17. Ito, Y.; Yanase, S.; Tokuda, H.; Kishishita, M.; Ohigashi, H.; Hirota, M.; Koshimizu, K., Epstein-Barr virus activation by tung oil, extracts of Aleurites fordii and its diterpene ester 12-O-hexadecanoyl-16-hydroxyphorbol-13-acetate. *Cancer letters* **1983,** *18* (1), 87-95.

18. Park, Y.-J.; Choe, Y.-h.; Kim, B.-S., Bovine viral diarrhoea (BVD) virus antiviral activity of Korean Tung Tree (Aleurites fordii) extracts in vivo. *Indian Journal of Animal Research* **2015,** *49* (6), 823-826.

19. Pei, Y.-H.; Kwon, O.-K.; Lee, J.-S.; Cha, H.-J.; Ahn, K.-S.; Oh, S.-R.; Lee, H.-K.; Chin, Y.-W., Triterpenes with Cytotoxicity from the Leaves of Vernicia fordii. *Chemical and Pharmaceutical Bulletin* **2013,** *61* (6), 674-677.

20. Kim, D.-e.; Jung, S.; Ryu, H. W.; Choi, M.; Kang, M.; Kang, H.; Yuk, H. J.; Jeong, H.; Baek, J.; Song, J.-H.; Kim, J.; Kang, H.; Han, S.-B.; Oh, S.-R.; Cho, S., Selective oncolytic effect in Epstein-Barr virus (EBV)-associated gastric carcinoma through efficient lytic induction by Euphorbia extracts. *Journal of Functional Foods* **2018,** *42*, 146-158.

21. Hirota, M.; Ohigashi, H.; Koshimizu, K., Piscicidal Constituents and Related Diterpene Esters from Aleurites fordii. *Agricultural and Biological Chemistry* **1979,** *43* (12), 2523-2529.

22. Pei, Y.-H.; Kim, J. W.; Kang, H.-B.; Lee, H.-K.; Kim, C.-S.; Song, H.-H.; Chin, Y.-W.; Oh, S.-R., Tigliane diterpene esters with IFN γ-inducing activity from the leaves of Aleurites fordii. *Bioorganic & medicinal chemistry letters* **2012,** *22* (6), 2318-2320.

23. van Meerloo, J.; Kaspers, G. J. L.; Cloos, J., Cell Sensitivity Assays: The MTT Assay. In *Cancer Cell Culture: Methods and Protocols*, Cree, I. A., Ed. Humana Press: Totowa, NJ, 2011; pp 237-245.

24. Bonora, E.; Targher, G.; Alberiche, M.; Bonadonna, R. C.; Saggiani, F.; Zenere, M. B.; Monauni, T.; Muggeo, M., Homeostasis model assessment closely mirrors the glucose clamp technique in the assessment of insulin sensitivity: studies in subjects with various degrees of glucose tolerance and insulin sensitivity. *Diabetes Care* **2000,** *23* (1), 57-63.

25. Kendall, D. M.; Riddle, M. C.; Rosenstock, J.; Zhuang, D.; Kim, D. D.; Fineman, M. S.; Baron, A. D., Effects of exenatide (exendin-4) on glycemic control over 30 weeks in patients with type 2 diabetes treated with metformin and a sulfonylurea. *Diabetes Care* **2005,** *28* (5), 1083-91.

26. Steinberg, S. F., Structural basis of protein kinase C isoform function. *Physiol Rev* **2008,** *88* (4), 1341-78.

27. Calle, R.; Ganesan, S.; Smallwood, J. I.; Rasmussen, H., Glucose-induced phosphorylation of myristoylated alanine-rich C kinase substrate (MARCKS) in isolated rat pancreatic islets. *Journal of Biological Chemistry* **1992,** *267* (26), 18723-18727.

28. Thorens, B., GLUT2, glucose sensing and glucose homeostasis. *Diabetologia* **2015,** *58* (2), 221-32.

29. Van de Velde, S.; Wiater, E.; Tran, M.; Hwang, Y.; Cole, P. A.; Montminy, M., CREB Promotes Beta Cell Gene Expression by Targeting Its Coactivators to Tissue-Specific Enhancers. *Molecular and Cellular Biology* **2019,** *39* (17), e00200-19.

30. Ratner, R. E., Controlling postprandial hyperglycemia. *Am J Cardiol* **2001,** *88* (6a), 26h-31h.

31. Yang, H.-W.; Son, M.; Choi, J.; Oh, S.; Jeon, Y.-J.; Byun, K.; Ryu, B. M., Ishige okamurae reduces blood glucose levels in high-fat diet mice and improves glucose metabolism in the skeletal muscle and pancreas. *Fisheries and Aquatic Sciences* **2020,** *23* (1), 24.

32. Sun, Q.; Nie, S.; Wang, L.; Yang, F.; Meng, Z.; Xiao, H.; Xiang, B.; Li, X.; Fu, X.; Wang, S., Factors that affect pancreatic islet cell autophagy in adult rats: evaluation of a calorie-restricted diet and a high-fat diet. *PLoS One* **2016,** *11* (3), e0151104.

33. Hu, X.; Chen, F., Exogenous insulin antibody syndrome (EIAS): a clinical syndrome associated with insulin antibodies induced by exogenous insulin in diabetic patients. *Endocr Connect* **2018,** *7* (1), R47-R55.

34. Vent, W., Duke, JA & Ayensu, ES, Medicinal Plants of China. 2 Vols. 705 S., 1300 Strichzeichnungen. Reference Publ., Inc. Algonac. Michigan, 1985. ISBN 0-917266-20-4. Preis: geb. m. Schutzumschlag $94, 95. *Feddes Repertorium* **1987,** *98* (7-8), 398-398.

35. Henquin, J. C., Regulation of insulin secretion: a matter of phase control and amplitude modulation. *Diabetologia* **2009,** *52* (5), 739.

36. Nakashima, S., Protein kinase C alpha (PKC alpha): regulation and biological function. *J Biochem* **2002,** *132* (5), 669-75.

37. Komatsu, M.; Schermerhorn, T.; Aizawa, T.; Sharp, G., Glucose stimulation of insulin release in the absence of extracellular Ca2+ and in the absence of any increase in intracellular Ca2+ in rat pancreatic islets. *Proceedings of the National Academy of Sciences* **1995,** *92* (23), 10728-10732.

38. Easom, R. A.; Hughes, J. H.; Landt, M.; Wolf, B. A.; Turk, J.; McDaniel, M. L., Comparison of effects of phorbol esters and glucose on protein kinase C activation and insulin secretion in pancreatic islets. *Biochem J* **1989,** *264* (1), 27-33.

39. Guillam, M. T.; Hümmler, E.; Schaerer, E.; Yeh, J. I.; Birnbaum, M. J.; Beermann, F.; Schmidt, A.; Dériaz, N.; Thorens, B., Early diabetes and abnormal postnatal pancreatic islet development in mice lacking Glut-2. *Nat Genet* **1997,** *17* (3), 327-30.

40. Poitout, V.; Hagman, D.; Stein, R.; Artner, I.; Robertson, R. P.; Harmon, J. S., Regulation of the insulin gene by glucose and fatty acids. *The Journal of nutrition* **2006,** *136* (4), 873-876.

41. Roche, E.; Maestre, I.; Martin, F.; Fuentes, E.; Casero, J.; Reig, J.; Soria, B., Nutrient toxicity in pancreatic β-cell dysfunction. *Journal of physiology and biochemistry* **2000,** *56* (2), 119-128.

42. MacDonald, M. J., Influence of glucose on pyruvate carboxylase expression in pancreatic islets. *Arch Biochem Biophys* **1995,** *319* (1), 128-32.